New geochemical and age data on the ophiolites from the Othrys area (Greece): implication for the Triassic evolution of the Vardar

NEW GEOCHEMICAL AND AGE DATA ON THE OPHIOLITES FROM THE OTHRYS AREA (GREECE): IMPLICATION FOR THE TRIASSIC EVOLUTION OF THE VARDAR OCEAN

Valerio Bortolotti*, Marco Chiari,✉, Marta Marcucci*, Adonis Photiades***, Gianfranco Principi*** and **Emilio Saccani°**

* *Dipartimento di Scienze della Terra, Università di Firenze, Italy.*
** *C.N.R., Istituto di Geoscienze e Georisorse, Unità di Firenze, Italy.*
*** *Institute of Geology and Mineral Exploration (IGME), Athens, Greece.*
° *Dipartimento di Scienze della Terra, Università di Ferrara, Italy.*
✉ *Corresponding author, e-mail: mchiari@geo.unifi.it.*

Keywords: *Radiolaria, basalt geochemistry, Hellenides, Triassic, Jurassic. Greece.*

ABSTRACT

This paper presents new radiolarian biostratigraphic and volcanic geochemical data for the Agoriani Mélange Unit and Fourka Unit, which represent the basal part of the Othrys ophiolitic nappe (central Greece). The Agoriani Mélange Unit is the base of the Othrys ophiolitic nappe, consists of a tectono-sedimentary mélange that is, in turn, tectonically overthrust by the Fourka Unit, which consists of basalt-radiolarian chert sequences. Geochemical data show that, in the study area, the Agoriani Mélange includes alkaline within-plate basaltic (WPB) and normal-type mid-ocean ridge (N-MORB) sequences in the pillow-facies, while the Fourka Unit mainly consists of normal-type mid-ocean ridge basaltic (N-MORB) sequences, as well as low-K tholeiitic (L-KT) sequences, both in occurring in the pillow-facies. Alkaline WPB have a clear enriched nature, with high concentration of high field strength elements (HFSE), relative enrichment in light (L-) rare earth elements (REE) with respect to heavy (H-) REE, and high Nb/Y (> 0.7), Ce/Y (> 1.5) Ta/Hf (> 0.35), Th/Yb (> 0.7) and Ta/Yb (> 0.3) ratios. N-MORB rocks have a more depleted nature with flat N-MORB normalized HFSE patterns, flat or slightly LREE depleted chondrite normalized REE patterns, and low Nb/Y (< 0.3), Ce/Y (< 0.5) Ta/Hf (< 0.1), Th/Yb (< 0.08) and Ta/Yb (< 0.05) ratios. L-KT basalts show an evident subduction-related geochemical signature exemplified by depletion of Ta, Nb, Zr, and Ti relative to other HFSE, slight LREE/HREE enrichment, and relative enrichment of Th with respect to Ta. Biostratigraphic data for the Fourka Unit show that radiolarites associated with N-MORBs were deposited, on the whole, in Middle and Late Triassic time. In particular the late Anisian - early Ladinian age found in one stratigraphic section represents the oldest age ever reported for a MORB sequence in the Hellenides. Radiolarites deposited over the L-KT basaltic sequence are early Carnian - middle Norian/Late Norian in age. The radiolarites associated with alkaline WPB in the Agoriani Mélange did not yield determinable radiolarians, while a radiolarite sequence in this mélange not associated with basalts is middle Bathonian to late Bathonian/early Callovian in age. The data presented in this paper provide new constraints on the early (Middle-Late Triassic) phase of evolution of the Vardar Ocean in the Hellenides. The MORBs are interpreted to have erupted during Middle-Late Triassic time, related to the initial opening of the Vardar oceanic basin. The L-KT basalts are interpreted to have erupted during Middle-Late Triassic time (i.e., in part contemporaneously with MORBs), in the ocean-continent transition zone adjacent to the rifted continental margin. Moreover, we speculate that the alkaline WPB have formed in oceanic seamounts or in the ocean-continent transition zone adjacent to the rifted continental margin.

INTRODUCTION

The determination of the age of the magmatic products with different composition occurring in the ophiolitic complexes is an important clue, as it allows to define the timing of the magmatic events, which allow, in turn, to reconstruct the geodynamic evolution of the oceanic basins in which ophiolites were generated. However, ophiolitic complexes are commonly strongly deformed and the sedimentary cover is usually associated to the underlying basaltic lavas through bedding-parallel thrusts. In this case, the dating of the basaltic lavas through the determination of the age of their sedimentary cover is uncertain. Thus, one major problem in dating the basalts is to find sections in which basalts are in stratigraphic contact with their sedimentary cover.

From many years our team addressed his researches for verifying the existence and the extension of a Triassic Tethyan oceanic basin along the Dinaric-Hellenic chain, as well as its geodynamic role in its successive orogenic evolution. From the beginning of the nineties, Triassic oceanic basalts were sporadically found in some localities (e.g., Pindos, Jones ad Robertson, 1991; Mirdita, Marcucci et al., 1994). This discovery was mainly due to the full development of the biostratigraphy using the radiolarian assemblages, which allowed dating of the radiolarian cherts linked to the basalts generally present in tectonic units at the base of the large ophiolitic masses, which are widespread all along the Dinarides-Hellenides. Up to now, we found Middle to Late Triassic basalts of mid-ocean ridge affinity (MORB) in the Mirdita zone of Albania (Chiari et al., 1996; Bortolotti et al., 1996; 2004a; 2006) and in the Argolis area of Greece (Bortolotti et al., 2003; Saccani et al., 2003). A short preliminary note (Bortolotti et al., 2005) reported the presence of MORB also in the Othrys Ophiolite nappe. At the same time, similar findings came from few localities in the Hellenides, such as Peloponnesus (Degnan and Robertson, 2006) and Evia (Euboea) Island (Danelian and Robertson, 2001).

In this work we present a detailed study on the biostratigraphy of the radiolarian cherts and on the geochemistry of the associated basalts of the Agoriani Mélange Unit and Fourka Unit, which form the base of the Othrys ophiolitic Nappe (central Greece). The samples, where collected in sections where stratigraphic relationships between volcanic rocks and radiolarian cherts can be established. The aim of this paper is to relate the tectono-magmatic significance and the age of the basal units of the Othrys ophiolite nappe, for verifying if also in this area, remnants of Triassic oceanic rocks are preserved. These new data could permit a more

detailed reconstruction of the Triassic events related to the early evolution of the Tethys oceanic basin.

GEOLOGIC SETTING

The Hellenic Orogenic Belt constitutes the southern portion of the Dinaric-Hellenic Chain. It consists of three tectono-stratigraphic domains, the Adria Continent (to the west), the Vardar Ocean, the Serbo-Macedonian and the Rhodope Massifs (to the east).

The Adria Continental Domain has been subdivided into four isopic zones or sub-domains (Fig. 1a), which represented, during the Mesozoic, a continuous succession of northwest-southeast trending platforms and basins (Bortolotti and Principi, 2005, with references therein). From west to east they are: Ionian, Gavrovo, Pindos, and Pelagonian sub-Domains. These domains, which during the Dinaric-Hellenic orogenesis were thrust westwards, composing a complex nappe pile, follow each other in continuity, suggesting that an oceanic domain in between most likely did not existed. To the east of the Pelagonian sub-Domain, (here interpreted as the easternmost portion of the Adria Continent, see Bortolotti et al., 2003, Bortolotti and Principi, 2005) from the Middle Triassic to the end of the Mesozoic, existed an oceanic domain, which is known as Vardar Ocean. The eastern border of this ocean was represented by the Serbo-Macedonian Massif and the Rhodope Massif, representing the southwestern border of the Europe Continent.

This simple paleogeographic scenario (see also Bortolotti and Principi, 2005, and references therein) is not accepted by all the researchers. Many researchers prefer to imagine, during a part of the Mesozoic times, the presence of two or more oceanic basins located along the Dinaric-Hellenic orogenic chain (e.g., Jones and Robertson, 1991; Doutsos et al., 1993; Beccaluva et al., 1994; Ross and Zimmermann, 1996; Robertson and Shallo, 2000; Dilek et al., 2007).

In the Othrys area (central Greece, Fig. 1a), three different successions crop out (Fig. 1b): (1) the Pindos sub-Domain (to the west), (2) the Pelagonian sub-Domain (to the east) and (3) the Vardar Oceanic Domain, represented by the Vardar ophiolite tectonic nappe, which tectonically overlie both the Pindos and Pelagonian successions. We can consider this nappe as composed of a pile of four tectonic units, which, from the base upwards, are:

1- the "Agoriani Mélange Unit" (Ferrière et al., 1988), which consists of a tectono-sedimentary mélange including slivers of cherty limestones, radiolarian cherts, ophiolitic blocks, ophiolite-derived turbidites and debris flows (olistotromes);

2- the "Fourka Unit" (Ferrière, 1975; 1982; Celet et al., 1980), which consists of thrust sheets and blocks of pillow lavas topped by (or locally interfingerig with) thin ribbon radiolarian cherts;

3- The "Metalleion Unit" (Ferrière 1975), which is composed of serpentinized mantle harzburgites with dunite pods and by rodingitized gabbro dykes. Locally, an amphibolitic level occurs at the base of this unit. The occurrence of mantle rocks typical of supra-subduction oceanic zones (SSZ), such as harzburgites (Saccani et al., 2004, and reference therein), suggests that this unit has been derived from a SSZ tectonic setting.

4- The "Mega Isoma Unit" (Ferrière, 1975), consisting of serpentinized plagioclase lherzolites, locally intruded by gabbro bodies, and with some amphibolite slivers at the base. The occurrence of lherzolites may suggest an origin of this unit either from a mid-oceanic tectonic setting or, alternatively, from the slightly depleted mantle portions of a SSZ setting (Saccani et al., 2004).

The whole thrust pile system is unconformably covered by Upper Cretaceous limestones, Paleocene flysch and Oligocene-Miocene molasse.

In the various ophiolitic sequences along the Dinaric-Hellenic belt it is commonly observed that SSZ harzburgites

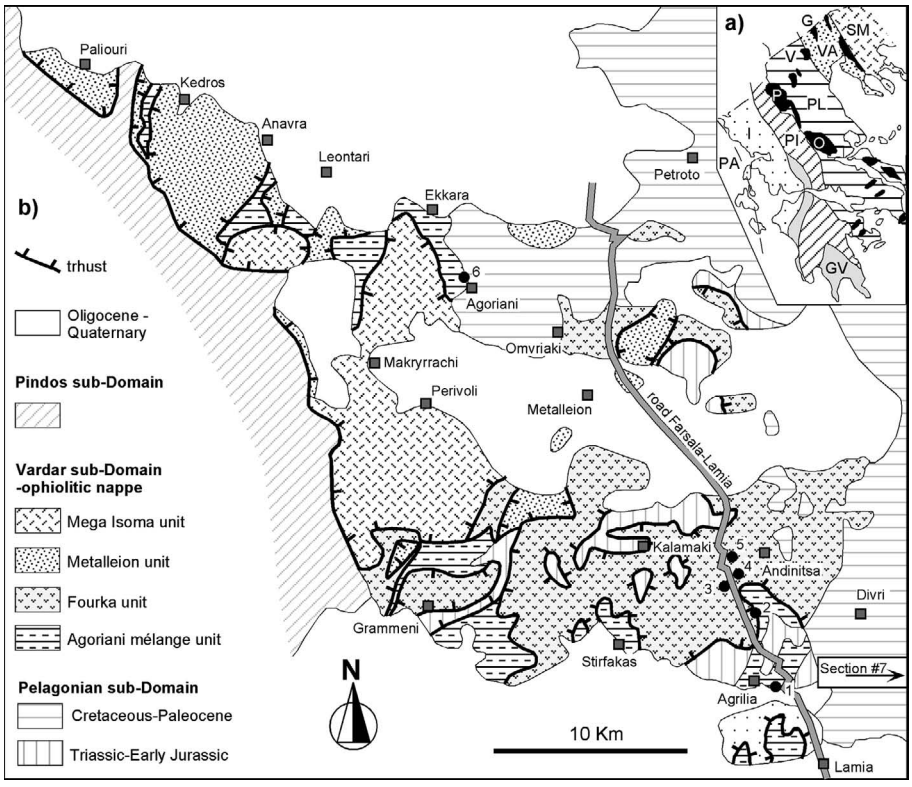

Fig. 1 - (a) Location of the Othrys massif and investigated area (box) with respect to the main tectono-stratigraphic zones of Greece (modified after Bortolotti et al., 2004b); (b) Geological sketch map of the southeastern Othrys area (modified after Ferrière, 1982). Abbreviations in Fig. 1a: PA- Pre-Apulian; I- Ionian; GV- Gavrovo; PI- Pindos; PL- Pelagonian; VA- Vardar; SM- Serbo-Macedonian; P- Pindos ophiolite; O- Othrys ophiolite; V- Vermion ophiolite; G- Guevgueli ophiolite. Dots and relative numbers indicate the location of the sections sampled for this work.

are trust onto lherzolites, representing, thus the top of the ophiolitic piles. By contrast, the Othrys ophiolitic massif represents the unique case in which lherzolites constitute the top of the ophiolitic pile.

SAMPLING AND FIELD OCCURRENCE

In order to investigate the age of the basalt-radiolarite succession and the geochemical variability of basalts in both the Agoriani Mélange Unit and Fourka Unit, 21 samples of basalts and 26 samples of radiolarian cherts were collected in 7 different outcrops located along the road from Lamia to Farsala (sections 1-5), the villages of Agoriani (section 6), and the village of Pelasghia (section 7) (Fig. 1b). Sections n. 1, 2 and 6 are representative of the Agoriani Mélange, whereas sections n. 3, 4, 5, and 7 are representative of the Fourka Unit.

The sampled basalts include pillow lavas, vesicular pillow lavas, and pillow breccias (Fig. 2); vesicular pillow lavas and pillow breccias were sampled where the amount of amygdales and calcite veins was minimum. The sampled cherts include only reddish ribbon cherts.

In sections n. 5 and 7 (Fourka Unit), the stratigraphic relationships of the basalts with the cherts have been clearly recognized. In the other sections, the radiolarite levels show more or less tectonized contacts with the basalts; nonetheless, field evidences suggest that the original sedimentary contacts have only been slightly displaced by tectonic processes.

Sections 1 and 2, located some km north of Lamia have been collected in the Agoriani Mélange, for comparison with the other ones coming from the Fourka Unit (the main object of this study):

Section 1 (Agoriani Mélange) located 3-4 km north of Lamia, where the Agoriani Mélange lies at the top of the Pelagonian limestones. In a large outcrop of basalts we collected six samples (1-6) in a space of about 100 m, and one sample from a cherty strip (GR84) included between the pillows (interpillow).

Section 2 (Agoriani Mélange) located 4-5 km north of Lamia, where we collected only three basaltic samples (7-9).

Section 3 (Fourka Unit) is located 5-6 km north of Lamia. In this section, we collected three basaltic samples (10-12) and three cherts (GR90-92) at their top, but the contact was strongly tectonized.

Section 4 (Fourka Unit) is located 7-8 km north of Lamia. We collected three basaltic samples (17-19) and five cherts (GR93-94 and 96-98). This section is very complex: the radiolarian cherts, with a tectonized contact with the basalts, are strongly deformed all along the section and include also a thick bed of reddish Mn-bearing limestone (GR95).

Section 5 (Fourka Unit) is located at some tens meters after the crossroad for the Antinitsi Monastery. In this section the stratigraphic relationships between the basalts and the overlying cherts are clear (Fig. 2). We collected four basaltic samples (13-16) and seven radiolarian cherts at their top (GR99-105).

Section 6 (Agoriani Mélange) is located near the village of Agoriani (Fig. 1b), along the road Ano Agoriani - Kato Agoriani. In this section no basalts are cropping out, thus we collected 9 chert samples (GR110-118).

Section 7 (Fourka Unit) is located near the village of Pelasghia, where the cherts stratigraphically cover the basaltic sequence. Here, we collected two basaltic samples (GR312-313) and one chert (GR314) at their top.

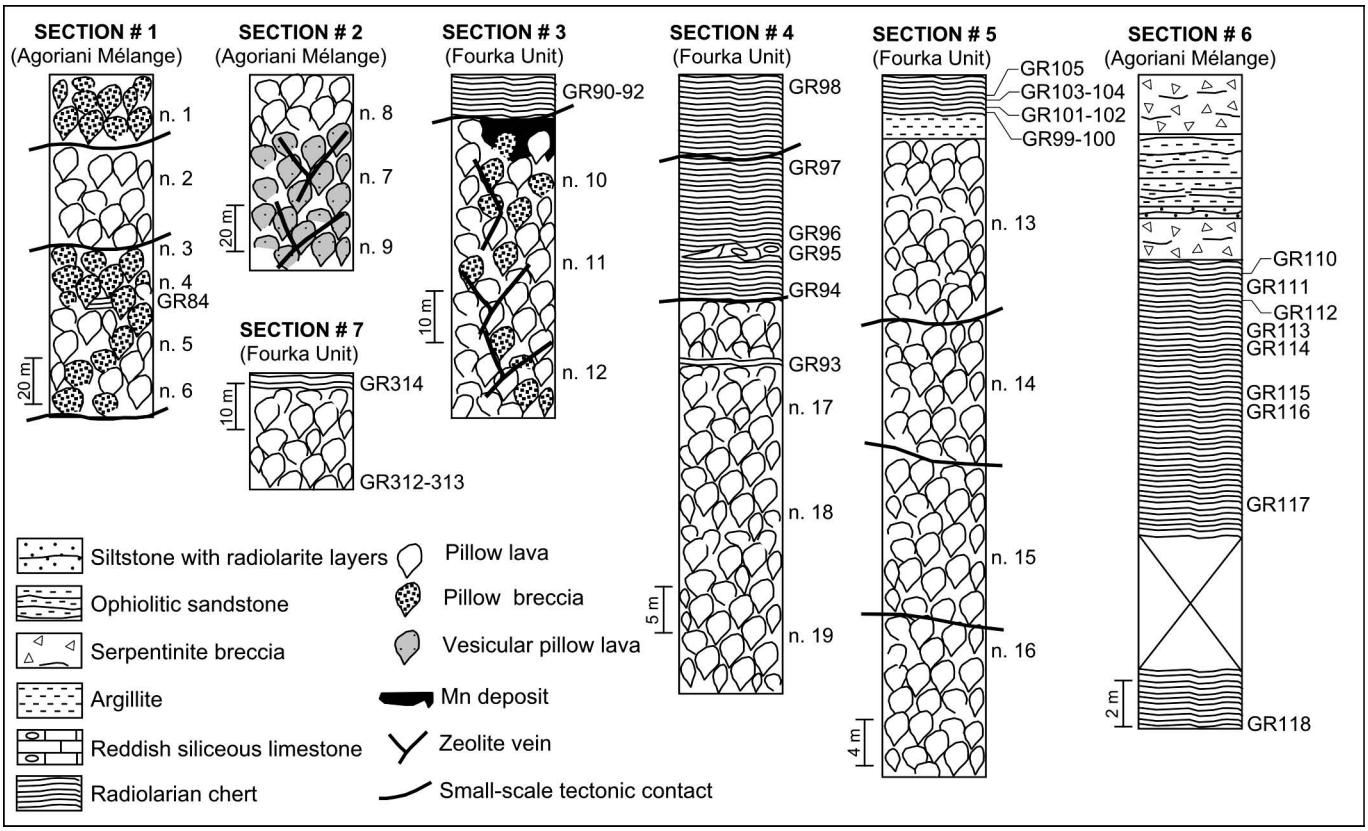

Fig. 2 - Simplified stratigraphic columns of the sampled sections (see Fig. 1 for location). The stratigraphic position of the radiolarian chert samples and volcanic rock samples is also reported.

PETROGRAPHY, GEOCHEMISTRY AND TECTONO-MAGMATIC SIGNIFICANCE OF BASALTIC ROCKS

Petrography

All the collected samples underwent variable degrees of ocean-floor hydrothermal alteration under static, greenschist facies conditions. This alteration has commonly resulted in intensive re-crystallization of the primary igneous phases, including the replacement of plagioclase by albite or clay minerals and the retrogression of clinopyroxene into chlorite or, subordinately, into actinolite-tremolite minerals. By contrast, the primary igneous textures are well preserved. The petrographic features of the analyzed samples are presented below according to the two different rock varieties recognized on chemical bases and described in the next section.

Group 1 basalts (high-Ti basalts). The pillow lava facies show various textures, including very fine-grained aphyric varieties with ophitic to sub-ophitic groundmasses, coarse-grained aphyric types characterized by plagioclase and poikilitic clinopyroxene, and slightly porphyritic types (PI < 10%), in which plagioclase phenocrysts are settled in sub-ophitic to intergranular groundmasses. The pillow breccia facies show monogenetic basaltic fragments in which all the texture types observed in the pillow facies are recognized. This volcanic facies is also characterized by abundant calcite veins. Pillow breccias from Section 3 have very high content of Fe-Ti oxides. In all samples groundmass mineral assemblage includes euhedral plagioclase and anhedral to interstitial clinopyroxene. Such a texture testifies for the early crystallization of plagioclase with respect to clinopyroxene. In few pillow lava samples small veins filled by chlorite occur.

Group 2 basalts (alkaline basalt). The pillow lava facies range in textures from aphyric to slightly porphyritic (PI < 10%), where phenocrysts are exclusively represented by plagioclase. Groundmass shows sub-ophitic, intersertal, and hyalophitic textures. Groundmass mineral assemblages include plagioclase, clinopyroxene, and opaque minerals. Vesicular pillow lavas have amygdales filled by calcite and chlorite. The pillow breccia facies display textures similar to those described above; nonetheless, hyalophitic textures are predominant. The volcanic glass is deeply altered and is replaced by a cryptocrystalline assemblage of clay minerals and chlorite. In addition, calcite veins are abundant.

Group 3 basalts (low-K tholeiitic basalts). These rocks are coarse-grained aphyric and show intergranular textures with euhedral clinopyroxene and sub-hedral plagioclase. Opaque minerals are abundant and sometimes are concentrated in veins or layers. Aggregates of secondary minerals most likely pseudomorph after olivine are also observed.

Analytical methods

Bulk-rock major and trace element analyses were performed by X-ray fluorescence (XRF) and by inductively coupled plasma-mass spectrometry (ICP-MS) at the Department of Earth Sciences of the University of Ferrara. Chemical compositions are presented in Table 1. The XRF analyses were performed on pressed powder pellets with an ARL Advant-XP automated spectrometer using the matrix correction methods proposed by Lachance and Trail (1966). The ICP-MS apparatus was a VG Elemental Plasma Quad PQ2 Plus spectrometer. Accuracy and detection limits were determined using a set of international standards. Accuracy for XRF analyses is better than 3% for Si, Ti, Ca, K and 7% for Al, Mn, Mg, Na, P, and better than 6% for trace elements, with the exception of Ba (8%), Th (10%), and Nb (13%). Detection limits for trace elements are: Zn, Cu, Sc, Ba = 5 ppm; Ni, Co, Cr, V, Rb = 1 ppm; Ga, Th, Nb, La, Sr, Zr, Y = 2 ppm. Accuracy for ICP-MS analyses ranges from 2 to 7 relative percent, with the exception of Nb (12%), Ta (16%), and U (9%). Detection limits (in ppm) are: Sc = 0.29; Nb, Hf, Ta = 0.02; Th, U = 0.01; light (L-) and medium (M-) rare earth elements (REE) < 0.07; heavy REE (HREE) < 0.13.

Volatiles were determined as loss on ignition (L.O.I.) at 1000°C, whereas CO_2 was determined by simple volumetric technique (Jackson, 1958) using standard amounts of reagent grade $CaCO_3$ and 11 reference samples with different CO_2 contents for calibration. The mean relative percentage error calculated using reference samples was 1.5%.

Geochemistry and tectono-magmatic interpretation

The petrographic analyses indicate that most of the samples underwent ocean-floor hydrothermal processes. These commonly lead to a variable mobilization of large ion lithophile elements (LILE), such as Ba, Rb, K, and Sr. By contrast, the transition metals (V, Cr, Mn, Fe, Co, Ni, Zn) and high field strength elements (HFSE) (Zr, Y, Nb, Ti, Hf, P) are relatively immobile, and largely reflect magmatic abundance (Pearce and Norry, 1979; Shervais, 1982; Pearce, 1983). REE are also relative immobile during alteration processes, although LREE may be slightly mobile when compared to HREE. The co-variation of Rb, Ba, K, and Sr with respect some HFSE (not shown) indicate that these elements have been largely mobilized in southeastern Othrys basalts. By contrast, Th, Ta, and, to a lesser extent, U plotted against HFSE indicate a scarce mobilization of these elements. For these reasons, the discussion on the geochemical and petrogenetic features of the studied rocks will be mainly based on those elements which can be considered immobile during metamorphic and alteration processes. In addition, due to the high amount of calcite in many of the studied samples, for the discussion of geochemical characteristics the major element composition of samples was re-calculated on calcite-free bases for a better comparison of chemical data. In detail, CaO in calcite has been calculated according to stoikiometric proportions with CO_2 contents, assuming, after the petrographic analyses, that the secondary carbonates are composed of calcite. The major element composition has then been re-calculated to 100 wt% without considering L.O.I. and CaO in calcite and these are the analyses we will be using from here on.

The data presented in this paper point out the occurrence of three geochemically distinct groups of lavas in the southeastern Othrys volcanic sequence.

Group 1 basalts (high-Ti basalt and Fe-basalt).

Group 1 basalts are represented by sample 2 of section 1 (Agoriani Mélange) and by samples of sections 3, 4 and 5 (Fourka Unit). They range in composition from basalts to Fe-basalt (Table 1) and display a clear sub-alkaline nature, as exemplified in Fig. 3. Basalts range in silica from 46.33 wt% to 51.08 wt%. MgO (5.64-9.87 wt%), CaO (8.63-11.76 wt%) contents, and Mg# (52.1-67.0), indicate that these studied samples represent volcanic products ranging from rather primitive to slightly evolved basalts. TiO_2 content is relatively high, ranging from 1.30 to 1.58 wt% and shows good positive

Table 1 - Bulk rock major and trace element analyses of basaltic rocks from the Agoriani Mélange Unit and Fourka Unit (southeastern Othrys ophiolite).

	Section 1 (Agoriani Mélange)											
Sample	1		2		3	4	5		6	
Rock	Bas		Bas		Bas	Bas	Bas		Bas	
Type	pillow breccia		pillow		pillow breccia	pillow breccia	pillow breccia		pillow	
Affinity	WPB		N-MORB		WPB	WPB	WPB		WPB	
	a	b	a	b	a	a	a	b	a	b
SiO_2	42.63		49.00		41.37	46.27	43.40		48.96	
TiO_2	1.12		1.26		0.96	1.10	1.03		1.04	
Al_2O_3	14.47		14.51		13.29	15.17	13.22		13.92	
Fe_2O_3	1.08		1.30		1.00	1.02	1.03		0.98	
FeO	7.20		8.66		6.65	6.77	6.84		6.51	
MnO	0.13		0.16		0.12	0.12	0.16		0.13	
MgO	7.52		9.87		8.45	7.10	10.44		8.06	
CaO	12.41		8.63		15.84	11.27	14.48		11.39	
Na_2O	3.08		3.43		2.32	3.25	2.52		3.14	
K_2O	1.63		0.40		1.19	1.60	0.30		1.12	
P_2O_5	0.28		0.12		0.22	0.22	0.18		0.21	
L.O.I.	8.37		2.67		8.65	6.17	6.41		4.63	
Total	99.93		100.01		100.06	100.05	100.01		100.09	
CO_2	3.38		nd		5.39	2.00	1.81		nd	
Mg#	65.1		67.0		69.4	65.2	73.1		68.8	
Zn	53		63		62	57	48		51	
Cu	37		109		30	73	65		67	
Sc	26	25.2	43	44.1	29	31	33	33.5	35	35.0
Ga	5		4		5	5	6		3	
Ni	154		19		161	140	159		163	
Co	31		43		42	33	39		42	
Cr	406		192		423	343	340		378	
V	240		276		252	285	300		305	
Rb	9	7.68	3	4.52	5	9	3	3.44	5	6.41
Ba	102		61		80	93	62		89	
Hf		1.87		2.18				1.84		1.82
Ta		0.71		0.14				0.72		0.69
Th	3	1.62	nd	0.14	3	nd	nd	1.47	2	1.41
U		0.27		0.05				0.33		0.23
Nb	12	13.2	3	4.39	12	13	13	11.7	11	11.1
Sr	99	102	259	264	145	112	162	191	188	191
Zr	66		75		59	67	64		63	
Y	19	17.5	24	23.4	22	19	18	17.7	19	18.0
La	15	12.6	4	3.71	15	16	14	12.8	13	12.1
Ce		26.5		9.30				27.7		25.0
Pr		3.18		1.53				3.26		3.14
Nd		12.7		7.46				13.3		12.8
Sm		2.85		2.46				2.94		3.01
Eu		0.87		0.83				0.82		0.82
Gd		2.75		3.18				2.72		2.68
Tb		0.50		0.58				0.50		0.51
Dy		3.27		4.15				3.28		3.19
Ho		0.69		0.92				0.70		0.69
Er		2.00		2.62				2.02		1.95
Tm		0.29		0.40				0.29		0.29
Yb		1.89		2.59				1.94		1.94
Lu		0.28		0.36				0.27		0.27
Ti/V	31		28		25	25	22		21	
Zr/Nb		5.0		17.0	4.9	5.2		5.4		5.6
Ta/Hf		0.38		0.06				0.39		0.38
$(La/Sm)_N$		2.85		0.97				2.81		2.58
$(Sm/Yb)_N$		1.68		1.06				1.68		1.72
$(La/Yb)_N$		4.78		1.03				4.72		4.45

Location of samples is reported in Figs. 1, 2. Abbreviations: Bas- basalt; Fe-Bas- Fe-basalt; WPB- within-plate basalt; MORB- mid-ocean ridge basalt; a- XRF analyses; b- ICP-MS analyses; nd- not detected. $Fe_2O_3 = 0.15 \times FeO$; $Mg\# = 100 \times Mg/(Mg + Fe^{2+})$, where Mg = MgO/40 and Fe = FeO/72. Normalizing values for REE ratios are from Sun and McDonough (1989).

Table 1 (*continued*)

	Section 2 (Agoriani Mélange)						Section 3 (Fourca Unit)			
Sample	7		8		9		10		11	12
Rock	Bas		Bas		Bas		Fe-Bas		Fe-Bas	Fe-Bas
Type	vesicular pillow		pillow		vesicular pillow		pillow breccia		pillow breccia	pillow brecci
Affinity	WPB		WPB		WPB		N-MORB		N-MORB	N-MORB
	a	b	a	b	a	b	a	b	a	a
SiO_2	44.56		45.91		45.17		35.30		26.11	26.29
TiO_2	1.24		1.19		1.09		1.50		1.25	0.99
Al_2O_3	16.32		15.61		15.71		11.35		10.11	9.52
$Fe2O_3$	0.97		1.08		0.99		1.56		2.75	2.25
FeO	6.48		7.17		6.61		10.42		18.33	14.98
MnO	0.17		0.16		0.13		0.17		0.17	0.18
MgO	8.89		6.81		7.22		3.45		3.40	2.56
CaO	9.57		10.01		10.21		19.57		21.54	25.39
Na_2O	3.80		4.59		4.55		2.66		1.61	1.55
K_2O	0.82		0.94		1.00		0.93		0.41	0.54
P_2O_5	0.24		0.21		0.24		0.14		0.13	0.11
L.O.I.	6.99		6.46		6.86		12.92		13.81	15.63
Total	100.05		100.13		99.78		99.96		99.60	99.98
CO_2	1.30		1.98		1.68		10.60		10.20	12.53
Mg#	71.0		62.9		66.1		37.1		24.8	23.3
Zn	72		64		75		54		44	29
Cu	40		64		59		23		17	37
Sc	32	32	31	27.6	30	25.9	31	35.3	26	22
Ga	6		4		4		7		10	12
Ni	176		131		157		33		19	7
Co	52		30		43		29		65	11
Cr	331		325		377		65		66	54
V	284		292		266		307		399	331
Rb	5	6.33	5	3.70	4	3.91	6	6.76	nd	2
Ba	95		90		84		71		46	38
Hf		2.10		1.89		2.01		2.90		
Ta		0.80		0.75		0.74		0.12		
Th	3	1.75	3	1.67	2	1.57	nd	0.15	nd	nd
U		0.33		0.29		0.27		0.09		
Nb	13	13.0	12	11.5	11	12.0	4	5.49	3	2
Sr	320	311	82	76	103	120	151	168	72	71
Zr	71		71		63		90		84	64
Y	19	19.5	19	20.1	19	19.0	34	32.5	27	22
La	11	12.9	15	13.7	13	11.6	6	4.36	13	11
Ce		28.3		28.1		25.4		11.9		
Pr		3.38		3.43		3.04		2.05		
Nd		13.6		13.2		12.5		10.7		
Sm		3.25		3.09		2.90		3.61		
Eu		0.89		0.90		0.87		1.17		
Gd		2.88		2.85		3.13		5.29		
Tb		0.52		0.52		0.56		1.04		
Dy		3.49		3.43		3.73		6.83		
Ho		0.77		0.73		0.81		1.57		
Er		2.16		2.10		2.30		4.45		
Tm		0.32		0.31		0.33		0.69		
Yb		2.11		2.03		2.16		4.40		
Lu		0.29		0.30		0.29		0.63		
Ti/V	28		26		26		34		22	21
Zr/Nb		5.5		6.1		5.2		16.4	28.0	32.2
Ta/Hf		0.38		0.40		0.37		0.04		
$(La/Sm)_N$		2.56		2.86		2.57		0.78		
$(Sm/Yb)_N$		1.71		1.69		1.49		0.91		
$(La/Yb)_N$		4.37		4.84		3.84		0.71		

Table 1 (*continued*)

	Section 4 (Fourca Unit)				Section 5 (Fourca Unit)							
Sample	17		18	19	13		14		15	16		
Rock	Bas		Bas	Bas	Bas		Bas		Bas	Bas		
Type	pillow		pillow	pillow	pillow		pillow		pillow	pillow		
Affinity	N-MORB		N-MORB	N-MORB	N-MORB		N-MORB		N-MORB	N-MORB		
	a	b	a	a	a	b	a	b	a	a	b	
SiO_2	46.32		48.69	47.46	51.08		49.20		42.84	35.28		
TiO_2	1.44		1.34	1.29	1.39		1.52		1.12	1.02		
$Al2O_3$	14.76		14.94	15.13	14.64		16.52		15.02	13.25		
Fe_2O_3	1.33		1.31	1.34	1.15		1.12		1.17	1.11		
FeO	8.86		8.73	8.95	7.68		7.48		7.81	7.43		
MnO	0.15		0.16	0.16	0.14		0.16		0.16	0.21		
MgO	9.71		9.05	8.25	7.80		6.85		4.94	4.54		
CaO	11.39		10.07	12.04	9.98		9.25		15.15	20.78		
Na_2O	2.60		2.99	2.74	3.88		3.67		3.30	2.99		
K_2O	0.02		0.22	0.06	0.07		0.29		0.28	0.14		
P_2O_5	0.13		0.11	0.12	0.10		0.15		0.11	0.10		
L.O.I.	3.36		2.43	2.66	2.15		3.83		7.72	13.06		
Total	100.07		100.04	100.20	100.06		100.04		99.62	99.91		
CO_2	0.60		nd	0.22	nd		nd		4.79	9.11		
Mg#	66.1		64.9	62.2	64.4		62.0		53.0	52.1		
Zn	65		59	56	70		75		49	42		
Cu	101		95	90	92		119		97	83		
Sc	44	41.5	43	41	43	40.5	49	45.1	34	29	47.0	
Ga	11		4	8	8		9		6	14		
Ni	33		42	35	26		32		53	39		
Co	42		37	39	41		49		57	46		
Cr	103		179	145	56		259		179	168		
V	299		280	276	316		311		235	190		
Rb	nd	0.75	nd	nd	nd	1.82	nd	1.11	nd	nd	1.73	
Ba	47		45	38	49		68		48	42		
Hf		2.64				2.45		2.34			2.02	
Ta		0.13				0.12		0.12			0.13	
Th	nd	0.18	nd	nd	nd	0.15	nd	0.14	nd	nd	0.17	
U		0.09				0.04		0.05			0.06	
Nb	5	5.63	2	3	3	4.36	2	2.97	nd	4	4.70	
Sr	42	51.0	137	51	140	136	254	262	201	109	115	
Zr	91		84	90	85		106		83	72		
Y	31	32.4	31	31	34	30.9	31	31.5	24	18	17.6	
La	5	4.72	4	2	5	3.66	5	3.56	6	4	3.89	
Ce		12.2				9.82		9.70			9.53	
Pr		1.88				1.53		1.52			1.48	
Nd		9.32				7.90		7.67			7.19	
Sm		3.13				2.72		2.69			2.24	
Eu		1.06				1.03		1.00			0.82	
Gd		4.09				3.65		3.69			2.91	
Tb		0.79				0.72		0.70			0.55	
Dy		5.66				5.32		4.89			3.68	
Ho		1.30				1.22		1.12			0.80	
Er		3.86				3.50		3.44			2.29	
Tm		0.56				0.53		0.52			0.35	
Yb		3.42				3.24		3.09			2.17	
Lu		0.47				0.45		0.42			0.33	
Ti/V	30		29	29	27		30		31	37		
Zr/Nb		16.2	41.8	30.0		19.4		35.7			15.3	
Ta/Hf		0.05				0.05		0.05			0.06	
$(La/Sm)_N$		0.97				0.87		0.85			1.12	
$(Sm/Yb)_N$		1.02				0.93		0.97			1.14	
$(La/Yb)_N$		0.99				0.81		0.83			1.28	

Table 1 (*continued*)

	Section 7 (Fourca Unit)			
Sample	GR312		GR313	
Rock	Bas		Bas	
Type	pillow		pillow	
Affinity	L-KT		L-KT	
	a	b	a	b
SiO_2	47.26		48.09	
TiO_2	0.53		0.60	
Al_2O_3	12.94		12.94	
Fe_2O_3	1.68		1.71	
FeO	11.18		11.39	
MnO	0.24		0.20	
MgO	9.97		11.14	
CaO	10.56		8.96	
Na_2O	3.47		3.28	
K_2O	0.93		1.00	
P_2O_5	0.05		0.06	
L.O.I.	1.12		0.69	
Total	99.93		100.06	
CO_2	nd		nd	
Mg#	61.2		63.6	
Zn	40		58	
Cu	29		38	
Sc	46	45.8	34	37.0
Ga				
Ni	225		273	
Co	28		48	
Cr	966		946	
V	142		164	
Rb	10	9.67	12	10.5
Ba	35		48	
Hf		1.53		1.70
Ta		0.05		0.05
Th		0.26		0.31
U		0.07		0.07
Nb	nd	1.19	1	1.74
Sr	121	128	126	123
Zr	19	22.3	24	27.7
Y	12	13.3	12	13.1
La	3	2.74	3	2.62
Ce		7.24		6.75
Pr		1.15		1.01
Nd		5.46		4.76
Sm		1.60		1.47
Eu		0.46		0.45
Gd		2.05		1.95
Tb		0.35		0.31
Dy		2.10		1.85
Ho		0.46		0.42
Er		1.32		1.14
Tm		0.18		0.17
Yb		1.22		1.16
Lu		0.17		0.17
Ti/V	24		23	
Zr/Nb		15.86		13.70
Ta/Hf		0.11		0.11
$(La/Sm)_N$		1.10		1.15
$(Sm/Yb)_N$		1.46		1.42
$(La/Yb)_N$		1.61		1.63

correlation with other incompatible elements including P_2O_5 (0.10 - 0.16 wt%), Zr (64-106 ppm), Y (18-34 ppm), and Nb (2.97-5.63 ppm). Basalts display generally low compatible element contents (Cr = 54-259 ppm, Ni = 7-53 ppm, Co = 11-65 ppm). Fe-basalts represent rather evolved magmatic products, as testified by their very low Mg# (23.3 - 37.1). The FeO_t content is exceptionally high (16.04 - 28.31 wt%) and the TiO_2 content is relatively high (1.52-2.08 wt%). Accordingly, the compatible element contents are low (Cr = 54-66 ppm, Ni = 7-33 ppm, Co = 11-65 ppm).

The distribution of HFSE concentrations (Fig. 4a) indicates that these rocks share affinities with ocean-floor basalts. In particular, elements from P to Yb exhibit rather flat patterns ranging from 0.7 to 1.5 times N-MORB (Sun and McDonough, 1989) contents. Accordingly, REE patterns (Fig. 4b) are consistent with N-MORB compositions, as they have both mild LREE depletion or enrichment (La_N/Sm_N = 0.78-1.12) and an overall enrichment for HREE of 10 - 30 times chondrite (Fig. 4b). Fe-basalts have the highest concentration of both incompatible elements and REE (Fig. 4a, b) and, in accordance with their relatively evolved nature, are characterized by moderate Eu negative anomaly (Fig. 4b).

The Ti/V ratios displayed by Group 1 basalts range from 21 to 37, which are typical values for basalts generated at mid-ocean ridge settings (Shervais, 1982). In the Th-Ta-Hf/3 discrimination diagrams of Fig. 5 Group 1 basalts plot in the fields for N-MORB composition.

Ratios of highly incompatible trace elements, such as Ce/Y and La/Yb, are generally little influenced by moderate extents of fractional crystallization, and are believed to reflect either the source characteristics or the degree of partial melting (Saunders et al., 1988). Ce and La are more incompatible than Y, and Yb, respectively; thus, rocks representing the smallest degree of partial melting or derived from more enriched sources exhibit both the highest Ce/Y and La_N/Yb_N ratios. These elemental ratios plotted in Fig. 6a for Group 1 basalts are very similar to those of modern primitive N-MORB (Sun and McDonough, 1989), and are generally compatible with a genesis from primary magmas originating from depleted N-MORB type sub-oceanic mantle sources, with no influence of enriched OIB-type material, as also confirmed by the Ta/Hf vs. La_N/Sm_N (Fig. 6b) and Th/Yb vs. Ta/Yb ratios plotted in Fig. 7. In addition, the N-MORB studied in this paper display many similarities with N-MORBs from various localities of the Hellenides (Saccani and Photiades, 2005, and references therein), as shown in Figs. 6 and 7. According to the models proposed by Pearce (1983), the Cr and Y composition of Group 1 basalts are compatible with 20% partial melting of a depleted MORB mantle source. Likewise, according to the model proposed by Haase and Devey (1996), their $(Dy/Yb)_N$ and $(Ce/Yb)_N$ compositions are compatible with 10-20% partial melting of a depleted MORB mantle source. In summary, the chemistry of Group 1 basalts points out for a generation in a mid-ocean ridge tectonic setting.

Group 2 basalts (alkaline basalts).

Group 2 basalts are represented by samples 1, 3, 4, 5, 6 of section 1 and by all samples of section 2 (Table 1), both sections represent the Agoriani Mélange. The Nb/Y and Zr/Y ratios (Fig. 3) evidence the transitional to alkaline nature of these rocks, which are exclusively represented by basalts (SiO_2 = 45.66 - 48.96 wt%). In general, they display quite uniform compositions and likely represent primitive or slightly evolved magmatic products, as evidenced by

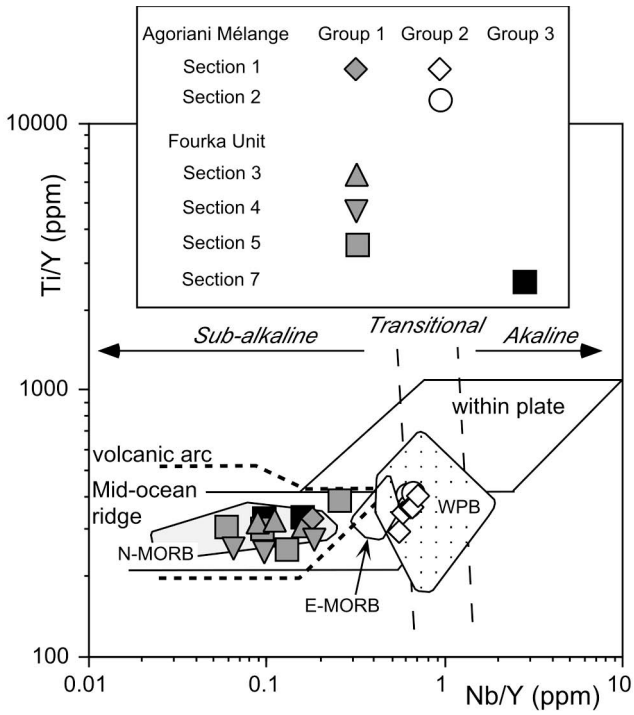

Fig. 3 - Ti/Y vs. Nb/Y diagram for basaltic rocks from the Agoriani Mélange Unit and Fourka Unit (southeastern Othrys ophiolite). Modified after Pearce (1982). Variations of elemental ratios of Triassic alkaline within-plate basalts (dotted field), as well as Triassic and Jurassic normal-type mid-ocean ridge basalts (N-MORB) (gray field) and enriched-type mid-ocean ridge basalts (E-MORB) (open field) from various localities of the Hellenides are reported for comparison (data from Saccani and Photiades, 2005, and references therein).

their relatively high Mg# (62.9 - 73.1), MgO (7.17 - 10.98 wt%), CaO (7.49 - 12.18 wt%), and P_2O_5 (0.19 - 0.31 wt%), as well as compatible element concentrations (Cr = 325 - 423 ppm, Ni = 131 - 176 ppm).

The incompatible element abundance (Fig. 4c) is characterized by a regularly decreasing pattern from Th to Yb; there is also a generalised enrichment with respect to MORB, particularly evident for LILE. The REE pattern (Fig. 4d) displays marked LREE enrichment with respect to HREE, exemplified by La_N/Yb_N ratios ranging from 3.84 to 4.84. The overall REE enrichment ranges from 10 to 60 times chondrite for Yb and La, respectively. These chemical features are comparable to those of typical within-plate alkaline basalts, such as ocean island basalts (OIBs) (Frey and Clague, 1983; Lipman et al., 1989; Haase and Devey, 1996). This conclusion is supported by the discrimination diagram of Fig. 5, where Group 2 basalts plot in the field for alkaline within-plate basalts.

The geochemistry of Group 2 basalts implies a derivation from a mantle source distinct from the depleted MORB-type mantle. OIB-like trace element and REE compositions suggest that these rocks represent magma generation associated with a plume-type geochemical component. The Ce/Y vs. La_N/Yb_N (Fig. 6a), Ta/Hf vs. La_N/Sm_N (Fig. 6b), and Th/Yb vs. Ta/Yb ratios (Fig. 7) indicate that these rocks were generated from an enriched mantle-type source without any detectable influence of continental crust contamination. The $(Dy/Yb)_N$ and $(Ce/Yb)_N$ ratios are compatible with 6-8% partial melting of a theoretical plume-type source (Haase and Devey, 1996).

The chemistry of these rocks is comparable with that of various Pacific seamounts (Frey and Clague, 1983; Lipman et al., 1989; Haase et al., 1997), as well as to that of transitional to alkaline rocks included in various ophiolitic mélange units of the Hellenides (Figs. 6 and 7). Many authors (e.g., Jones and Robertson, 1991; Pe-Piper, 1998; Saccani et al., 2003, Saccani and Photiades, 2005) suggested that transitional to alkaline basalts in the Hellenide mélanges were originated in intraplate oceanic island settings. Nonetheless, voluminous Lower-Middle Triassic alkali basalts, which are associated to the Permo-Triassic continental rifting of Gondwana are found in the Pelagonian continental margin (e.g., Pe-Piper, 1998). Based on a comparison with the overall geological characteristics of these different Triassic alkaline basalts, it can be assumed that Group 2 alkaline basalts from the Othrys area most likely represent seamount material or volcanic rocks erupted at the ocean-continent transition zone.

Group 3 basalts (Low-K tholeiitic basalts).

Group 3 rocks are found in samples GR312 and GR313 of section 7 (Fourka Unit) are represented by basalt with SiO_2 concentrations between 47.26 and 48.09 wt% and Mg# between 61.29 and 63.9 (Table 1). As distinctive features, these rocks have high MgO contents (9.97 - 11.14 wt%), low TiO_2 (0.53 - 0.60 wt%), Al_2O_3 (12.94 wt%) contents and very low Zr (19 - 24 ppm) and Y (12 ppm) contents. These rocks are also characterized by exceptionally high Cr contents (946 - 966 ppm).

In Fig. 3 they exhibit a clear sub-alkaline affinity, having Nb/Y ratios ranging from 0.1 to 0.2. Incompatible element patterns (Fig. 4e) are significantly depleted in HFSE with respect to normal-type MORB (N-MORB) and show high Th concentrations, La and Ce positive anomalies, and Ta, Nb, P, Zr, Ti negative anomalies. The chondrite-normalized REE patterns (Fig. 4f) are regularly decreasing from LREE to HREE and are characterized by slight LREE enrichment, with La_N/Yb_N ratios ranging from 1.61 to 1.63. In addition, both samples display Eu negative anomalies.

The incompatible element and REE abundance (Fig. 4e, f) exhibit patterns, which are very similar to those of oceanic low-K tholeiitic basalts of the orogenic series (Pearce, 1983). Accordingly, in the discrimination diagrams shown in Fig. 5, these rocks plot in the fields for calc-alkaline basalts. Triassic basaltic rocks from the Othrys region that are for many aspects similar to the Group 3 basalts have been described by Capedri et al. (1997). They are characterized by low Ti, very low Zr and Y, and very high Cr contents, as well as similar REE patterns, but, differently from Group 3 basalts, they have high Nb and LFSE (low field strength element) concentrations and were interpreted as E-MORBs On the bases of the overall geochemical features, particularly the HFSE depletion with respect to N-MORB, Group 3 basalts can be interpreted as low-K tholeiites.

The incompatible element and REE distribution of low-K tholeiitic rocks (Fig. 4e, f) indicates that they originated from a depleted mantle source further enriched by a subduction component. In particular, this subduction component is shown by the marked enrichment in Th with respect to Ta (Fig. 7).

No similar rocks have been found yet in the Hellenides. Nonetheless, Triassic calc-alkaline volcanic rocks have been described in several localities of the Hellenides (Capedri et al., 1997; Pe-Piper, 1998, and references therein). These are interpreted as having originated in a continental extensional setting from a mantle source bearing subduction-related

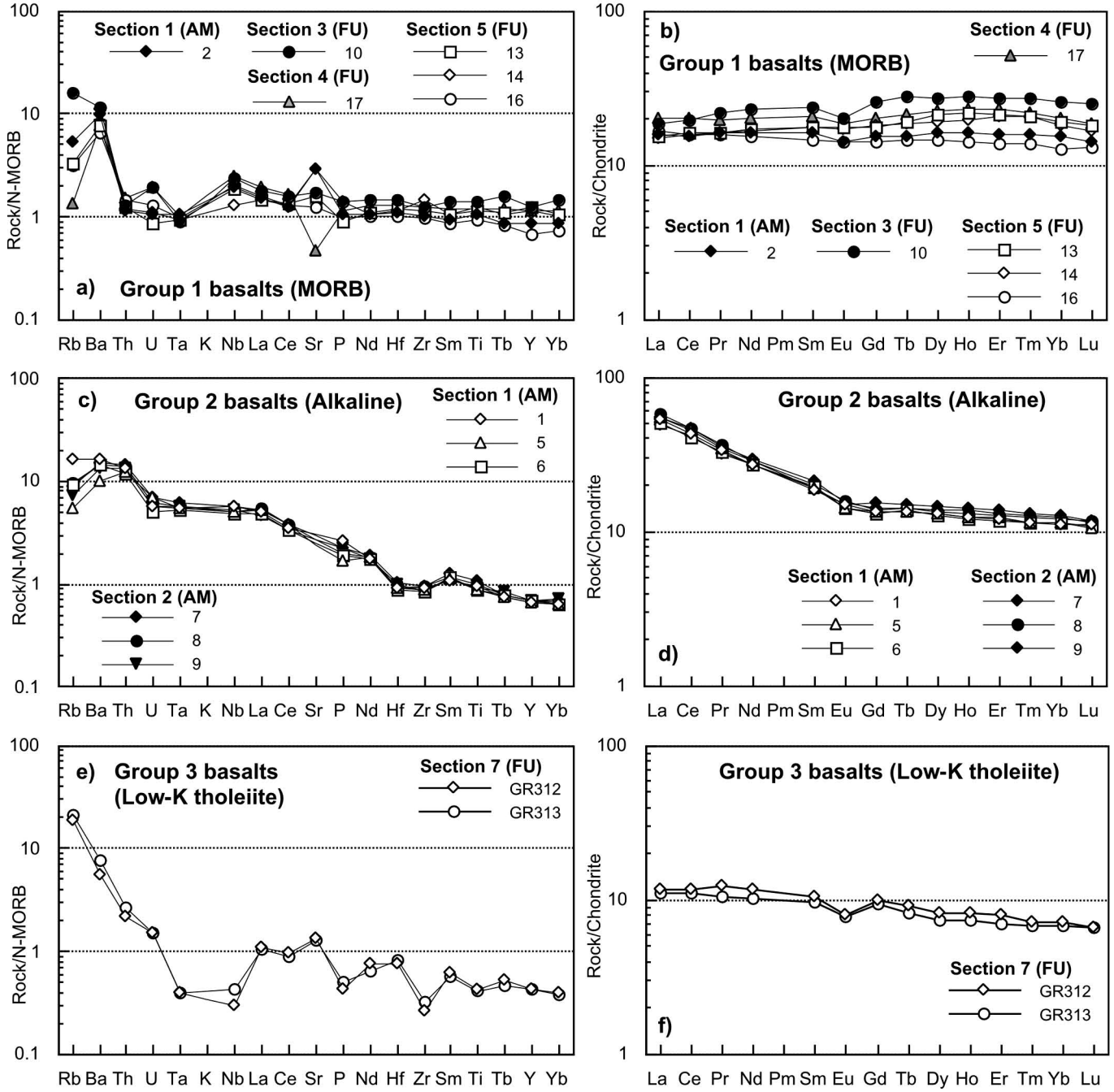

Fig. 4 - N-MORB normalized incompatible element (a, c, e) and chondrite-normalized REE (b, d, f) patterns for Group 1 (mid-ocean ridge basalts), Group 2 (alkaline basalts), and Group 3 (low-K tholeiitic basalts) from the Agoriani Mélange (AM) and Fourka Unit (FU), southeastern Othrys ophiolites. Normalizing values are from Sun and McDonough (1989).

geochemical characteristics inherited from a Hercynian subduction below Gondwana (Pe-Piper, 1998). This extensional setting is associated with the Permian-Triassic extension of the continental crust, which preceded the Vardar oceanic spreading. In lack of any other evidence, a similar tectonomagmatic environment of formation can reasonably be postulated for the Group 3 low-K tholeiitic basalts studied in this paper.

BIOSTRATIGRAPHY

Methods

Radiolarians have been extracted from cherts using differential HF attack, according to the method introduced by Dumitrica (1970), and Pessagno and Newport (1972). For the Middle and Upper Triassic radiolarian markers we utilize the ranges proposed by Dumitrica (1978), Lahm (1984), Goričan and Buser (1990), Ramovs and Goričan (1995), Sashida et al. (1999), Tekin (1999) Feng et al. (2001), Kozur and Mostler (1994), Goričan et al. (2005), Tekin and Mostler (2005) and Tekin and Bedi (2007). For the Middle Jurassic markers we utilize the zonation, based on the Unitary Association Zones (UAZ.), of Baumgartner et al. (1995a) and the ranges reported in Prela et al. (2000), Dumitrica and Dumitrica-Jud (2005) and Chiari et al. (2008). The age results are synthetically presented in Fig. 8.

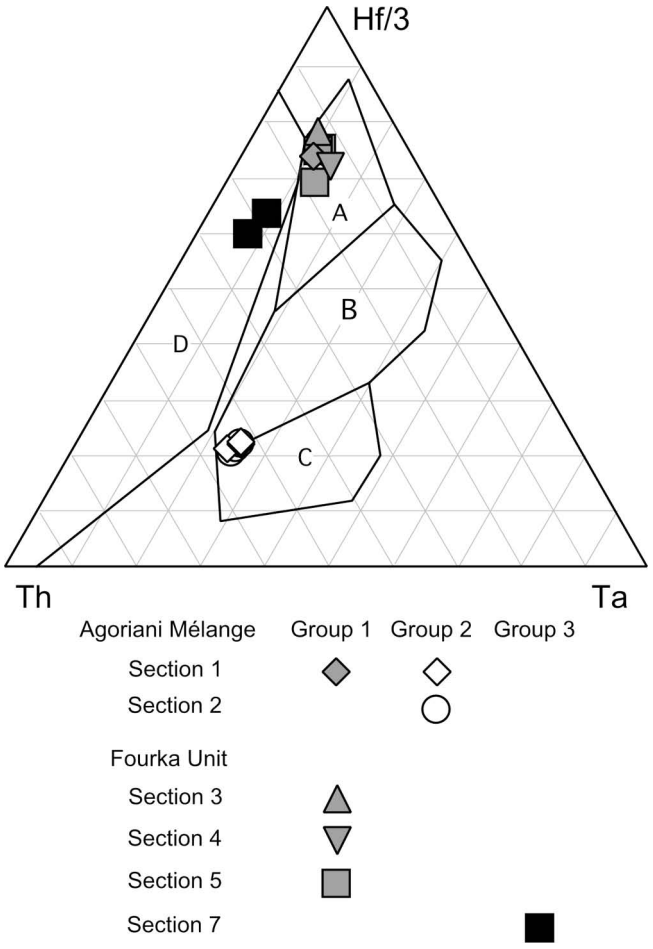

Fig. 5 - Th, Ta, Hf/3 (Wood, 1980) discrimination diagram for volcanic rocks from the Agoriani Mélange Unit and Fourka Unit (southeastern Othrys ophiolites). Fields, A: normal-type mid-ocean ridge basalts (N-MORB); B: enriched-type mid-ocean ridge basalts (E-MORB) and within-plate tholeiites; C: within-plate alkaline basalts; D: calc-alkaline basalts.

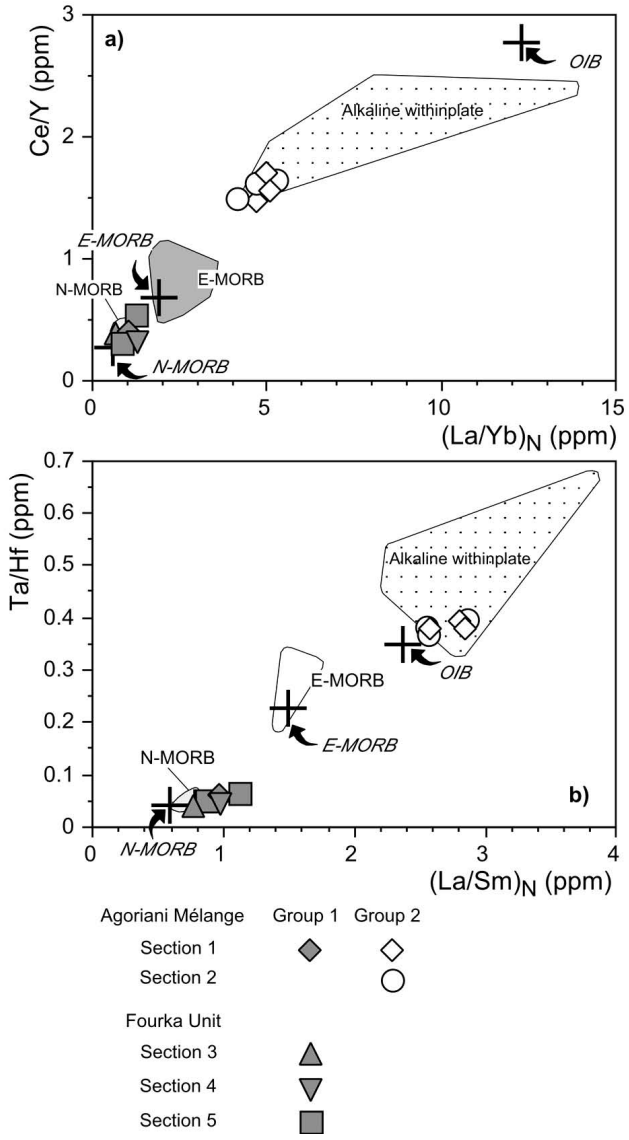

Fig. 6 - (a): Ce/Y vs. $(La/Yb)_N$ and (b): Ta/Hf vs. $(La/Sm)_N$ diagrams for basaltic rocks from the Agoriani Mélange Unit and Fourka Unit (southeastern Othrys ophiolites). Compositions of Modern ocean-island basalt (OIB), enriched-type mid-ocean ridge basalt (E-MORB), and normal-type mid-ocean ridge basalt (N-MORB) are from Sun and McDonough (1989). Variations of elemental ratios of Triassic alkaline within-plate basalts (dotted field) and Triassic-Jurassic N-MORBs (gray field) and E-MORBs (open field) from various localities of the Hellenides are reported for comparison (data from Saccani and Photiades, 2005, and references therein).

Fourka Unit

Section 3 - (Fig. 2).

The sample GR91 (Plate 1: 3, 10, 15), collected at the tectonized contact with the pillow basalts gave a radiolarian assemblage with *Capnuchosphaera* sp., *Pseudostylosphaera nazarovi* (Kozur and Mostler) and spines of *Spongotortilispinus tortilis* (Kozur and Mostler). The age is early-middle Carnian (Late Triassic), for the presence of *Capnuchosphaera* sp. (range: early Carnian - middle Norian/?late Norian, in Tekin, 1999) and *Pseudostylosphaera nazarovi* (range: late Ladinian - middle Carnian, in Tekin, 1999)

Section 4 - (Fig. 2).

The radiolarian cherts GR93-94 did not yield determinable radiolarians. The sample GR97 (Plate 1: 5, 6), collected about 15 metres from the tectonized contact with the pillow basalts, contains the following species: *Archaeocenosphaera* sp., *Capnuchosphaera* sp., *Corum* (?) sp., *Cryptostephanidium* (?) sp. and spines of *Spongotortilispinus tortilis* (Kozur and Mostler). The presence of *Capnuchosphaera* sp. (range: early Carnian - middle Norian/?late Norian, in Tekin, 1999) and *Spongotortilispinus tortilis* (Kozur and Mostler) (range: late Ladinian – early Norian, in Tekin, 1999) indicates an early Carnian - early Norian age (Late Triassic). The sample GR98 (Plate 1: 2, 19), collected about 23 metres from the tectonized contact with the pillow basalts, contains *Capnodoce* sp. and *Xiphothecaella* sp. cf. *X. karpenissionensis* (De Wever). The presence of *Capnodoce* sp. (range: late Carnian - late Norian, in Tekin, 1999 and Sashida et al., 1999) and the genus *Xiphothecaella* (range: middle Carnian - early Norian or middle Carnian - ?middle Norian, in Tekin, 1999 and Tekin and Bedi, 2007) indicates a late Carnian - early Norian age (or late Carnian - ?middle Norian) (Late Triassic).

Section 5 (Fig. 2).

This thin sequence of radiolarites at the top of the basalts gave badly preserved radiolarian assemblages of Triassic age; only the sample GR104 (Plate 1: 1, 7-9, 11-14, 16-18),

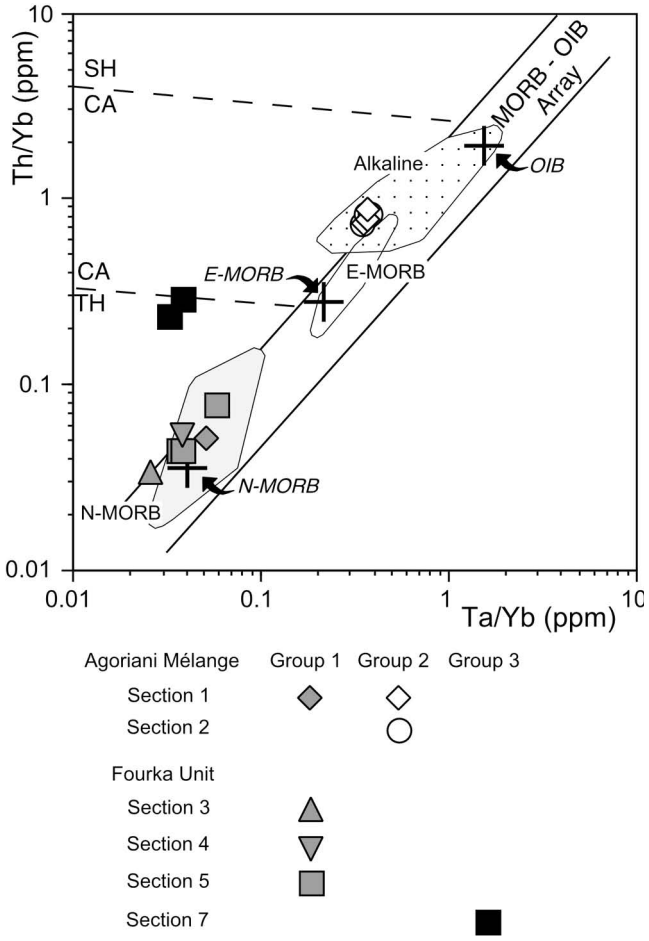

Fig. 7 - Th/Yb vs. Ta/Yb diagram for basaltic rocks from the Agoriani Mélange Unit and Fourka Unit (southeastern Othrys ophiolite). Compositions of Modern ocean-island basalt (OIB), enriched-type mid-ocean ridge basalt (E-MORB), and normal-type mid-ocean ridge basalt (N-MORB) are from Sun and McDonough (1989). Variations of elemental ratios of Triassic alkaline within-plate basalts (dotted field) and Triassic-Jurassic N-MORBs (gray field) and E-MORBs (open field) from various localities of the Hellenides are reported for comparison (data from Saccani and Photiades, 2005, and references therein).

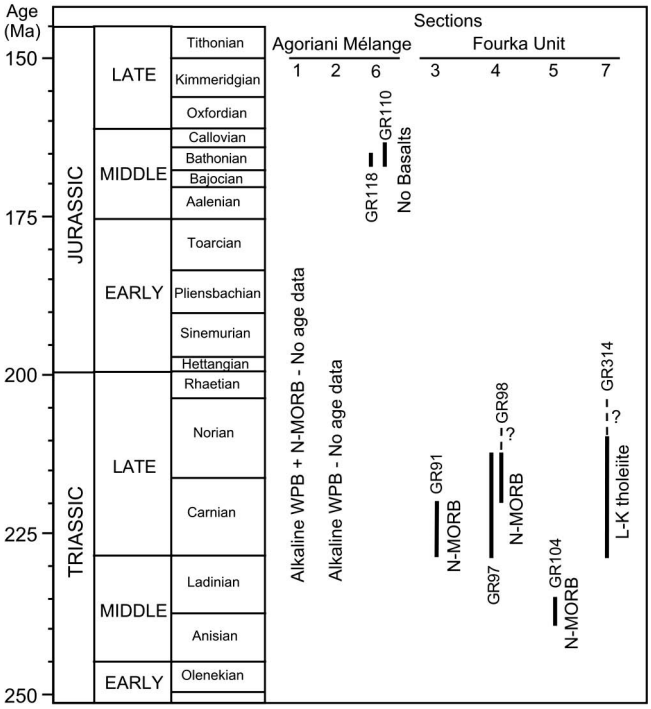

Fig. 8 - Summary of the biostratigraphic and geochemical evidences for the basaltic and radiolarian chert sequences in the Agoriani Mélange Unit and Fourka Unit (southeastern Othrys ophiolite). Abbreviations, WPB: within-plate basalt; N-MORB: normal-type mid-ocean ridge basalt; L-K: low-K.

collected about 3.10 metres form the pillow basalts, yield a well preserved radiolarian assemblage containing *Archaeocenosphaera* sp., *Eptingium manfredi robustum* Kozur and Mostler, *Pseudostylosphaera* sp. cf. *P. japonica* (Nakaseko and Nishimura), *Parasepsagon* sp. cf. *P. tetracanthus* Dumitrica, Kozur and Mostler, *Pseudostylosphaera canaliculata* (Bragin) (= *Pseudostylosphaera coccostyla* (Rüst)), *Spongostephanidium spongiosum* Dumitrica, *Spongoxystris koppi* (Lahm), *Spongoxystris tetrapterum* (Ramovs and Goričan), *Triassistephanidium* sp. cf. *T. laticornis* Dumitrica, *Triassospongosphaera* sp., *Vinassaspongus* (?) sp., *Weverisphaera* sp.

The age is referable to a late (or latest) Anisian - early Ladinian age (Middle Triassic) for the presence of *Eptingium manfredi robustum* (early Fassanian-middle Fassanian in Kozur and Mostler 1994), *Pseudostylosphaera canaliculata* (= *Pseudostylosphaera coccostyla*, range: Anisian - late Ladinian in Sashida et al., 1999 and Tekin, 1999), *Spongostephanidium spongiosum* (range: early Ladinian - ?Carnian in Dumitrica, 1978 and Goričan et al., 2005), *Spongoxystris koppi* (range: Anisian to Ladinian in Tekin and Mostler, 2005 and Sashida et al., 1999) and *S. tetrapterum*. (range: late Illyrian - ?earliest Ladinian, in Ramovs and Goričan, 1995).

Section 7 (Fig. 2).

Only in the sample GR314, collected, at about from 20 metres from the basalts GR312-313, we found radiolarians (not well preserved). The presence of *Capnuchosphaera* (?) sp. (Plate 1: 4) could indicate an early Carnian - middle Norian/?late Norian (Late Triassic) (range: *Capnuchosphaera* sp., in Tekin, 1999).

Agoriani Mélange

Section 1 - (Fig. 2).

The collected sample (GR84) did not yield determinable radiolarians.

Section 6 - (Fig. 2).

Radiolarian assemblages in a chert succession in sedimentary contact with ophiolitic sandstones and breccias. The sample GR118 (Plate 2: 2, 4, 5, 9, 12, 13, 15, 18, 21), collected near the base of the section, contains *Archaeodicyomitra* (?) *amabilis* Aita, *Eucyrtidiellum ptyctum* (Riedel and Sanfilippo), *Eucyrtidiellum* sp., *Kilinora spiralis* gr. (Matsuoka), *Stichocapsa robusta* Matsuoka, *Striatojaponocapsa conexa* (Matsuoka), *Striatojaponocapsa synconexa* O'Dogherty, Goričan and Dumitrica, *Unuma gordus* Hull, *Zhamoidellum* sp. cf. *Z. ovum* Dumitrica. The age is middle Bathonian (UAZ. 6) due to the occurrence of *Kilinora spiralis* gr. (range: UAZ. 6-8, in Baumgartner et al., 1995b and Chiari et al., 2008) with *Striatojaponocapsa synconexa* (range: UAZ. 4-6, in Baumgartner et al., 1995b and Prela et al., 2000) and *Unuma gordus* (range: UAZ. 4-6, in Baum-

gartner et al., 1995b).

The sample GR110 (Plate 2: 1, 3, 6-8, 10, 11, 14, 16, 17, 19, 20), collected about 19 metres from the sample GR118, contains *Angulobracchia* (?) sp., *Dictyomitrella kamoensis* Mizutani and Kido, *Eucyrtidiellum ptyctum* (Riedel and Sanfilippo), *Gongylothorax sakawaensis* Matsuoka, *Gorgansium* spp. sensu Baumgartner et al. (1995a), *Hexasaturnalis minor* (Baumgartner), *Podobursa* sp., *Pseudodictyomitrella* sp. cf. *P. tuscanica* (Chiari, Cortese and Marcucci), *Saitoum* sp., *Stichocapsa convexa* Yao, *Stichocapsa robusta* Matsuoka, *Striatojaponocapsa plicarum* s.l. Yao, *Transhuum maxwelli* gr. (Pessagno), *Triactoma* sp. cf. *T. jonesi* (Pessagno), *Tritrabs casmaliaensis* (Pessagno), *Unuma* sp. cf. *U. gordus*, *Williriedellum* sp. cf. *W. carpathicum* Dumitrica, *Zhamoidellum* sp. aff. *Z. argandi* O'Dogherty, Goričan and Dumitrica. The age is middle Bathonian to late Bathonian/early Callovian (UAZ. 6-7) due to the occurrence of *Gongylothorax sakawaensis* (range: UAZ. 6-7 in Baumgartner et al., 1995b), *Hexasaturnalis minor* (range: middle Bathonian - latest Tithonian/early Berriasian in Dumitrica and Dumitrica-Jud, 2005) with *Dictyomitrella kamoensis* (range: UAZ. 3-7, in Baumgartner et al., 1995b) and *Stichocapsa robusta* (range: UAZ. 5-7, in Baumgartner et al., 1995b).

DISCUSSION AND CONCLUSIONS

The age of the magmatic rocks included in the Agoriani Mélange cannot be constrained either because no complete stratigraphic sequences are found or because radiolarian cherts did not yield determinable radiolarians. Nonetheless, the middle Bathonian to late Bathonian/early Callovian age of the radiolarian cherts (linked with ophiolitic sandstones) of section 6 suggests that at this time ophiolitic rocks (mainly mantle serpentinites) were eroded and that in the Othrys area a mélange was already forming. Beside the occurrence of alkaline within-plate and MORB rocks described in this paper (sections 1 and 2, Fig. 8), Saccani and Photiades (2005) have shown that elsewhere the Agoriani Mélange also include volcanic rocks generated in a SSZ setting, such as boninitic rocks and basalts with geochemical characteristics intermediate between MORB and low-Ti island arc tholeiites (medium-Ti basalts of Saccani et al., 2004). This suggests that the Agoriani Mélange incorporated various material from different tectonic settings, that are: MORB from the oceanic setting, alkaline WPB from seamounts or from the ocean-continent transition zone, as well as boninites and medium-Ti basalts from the SSZ setting.

By contrast, the age of the magmatic rocks included in the Fourka Unit can be clearly constrained. The age of the MORB rocks range, on the whole, from Middle to Late Triassic. In particular, the late Anisian-early Ladinian age determined in section 5 (Fig. 8) is the oldest age ever found for MORB rocks in the Hellenides. In addition the Fourka Unit includes Low-K tholeiites of Late Triassic age (section 7, Fig. 8), whose occurrence has never been described before in literature.

The data presented in this paper are too limited for allowing the development of a tectonic model for the evolution of the Vardar Ocean in the Othrys area. Nonetheless, the new data presented herein can be used to integrate, for the Triassic time span, the models already presented in the literature.

Several models for the tectono-magmatic evolution of the Mesozoic branch of the Tethys in the Hellenide sector have previously been suggested by some authors (e.g., Robertson et al., 1996; Robertson, 2002; Bortolotti et al., 2005; Bortolotti and Principi, 2005; Saccani and Photiades, 2005; Sharp and Robertson, 2006). These are based on the occurrence of Triassic magmatic rocks from various tectonic zones of the Hellenides (Pe-Piper, 1998; Pe-Piper and Piper, 2002); the occurrence of a large variety of volcanic rocks of various ages (from Triassic to Jurassic) in the tectonic- sedimentary mélanges that are entrained beneath and within the different ophiolitic complex scattered throughout the Hellenide chain (Jones and Robertson, 1991; Saccani and Photiades, 2005); and on the characteristics of the Jurassic ophiolites (see Saccani et al., 2004 for a complete review). Regardless of the existence of one (Bortolotti et al., 2005, and references therein) or two (e.g., Jones and Robertson, 1991; Doutsos et al., 1993; Beccaluva et al., 1994; Ross and Zimmermann, 1996; Robertson and Shallo, 2000; Dilek et al., 2007) oceanic basins located between the Adria and European continental margins, these models can be integrated and summarized as follows.

From the Late Paleozoic - Early Triassic, the extensional tectonics that affected the Gondwana trigged the rifting of the continental lithosphere between the forthcoming Adria and European plates. The magmatic activity associated to this phase was dominated by the formation of shoshonitic and calc-alkaline series (Bébien et al., 1978; Pe-Piper, 1998), whose subduction-related geochemical characteristics were inherited from a former (Hercynian) subduction below Gondwana, which chemically modified the sub-continental lithospheric mantle through hydration processes and metasomatic enrichment in LILE, LREE, and Th (Pe-Piper, 1998). In the absence of other evidences (i.e., the existence of an Upper Triassic volcanic arc in this region), the Middle-Upper Triassic low-K tholeiitic basalts of the Fourka Unit, having clear subduction-related geochemical features can most likely be associated with this type of magmatism. If this assumption is correct, two possible interpretations can be postulated for this low-K tholeiitic magmatism. (1) The magmatism with subduction-related imprinting was not limited to the upper Paleozoic - Lower Triassic rifting-drifting stage, as previously reported in literature (e.g., Pe-Piper, 1998), but may have continued up to the Late Triassic (Fig. 8). (2) The low-K tholeiitic basalts of the Fourka Unit may represent an example of "delayed" magmatism occurred at passive margins. Some examples of "delayed" magmatism are found in the Eastern Atlantic passive margin, where small volumes of alkaline magmas were erupted in both continental and offshore settings some tens Ma after the rift-drift event (Rocchi et al., 2007a). This magmatism is interpreted as the result of the reactivation of the former mantle source in consequence of tectonic events (Rocchi et al., 2007b) linked to the ocean fracture zones. According to this interpretation, the low-K tholeiitic basalts of the Fourka Unit may thus be associated with the reactivation of the subduction-modified mantle source that was active during the Permo-Triassic rifting. Field evidences suggest that these rocks were erupted in an oceanic environment; therefore such reactivation most likely occurred in the ocean-continent transition zone. The rifting phase was also associated with the eruption of chemically enriched alkaline basalts suggesting that an OIB-type mantle source had been active since the Early(?)-Middle Triassic (Jones and Robertson, 1991; Pe-Piper, 1998; Saccani and Photiades, 2005).

The persisting extension between Adria and Europe (or in the NE border of Gondwana?) lead to the uprising of primitive asthenosphere and generation of the early oceanic crust starting from the Middle Triassic (Bortolotti et al., 2003). Variable interaction between the uprising primitive

asthenosphere and the OIB-type mantle source resulted in the generation of E-MORBs as the oceanic basin formed (Saccani and Photiades, 2005).

Subsequently, the oceanic crust evolved to N-MORB composition in consequence of partial melting of pure sub-oceanic mantle (Saccani et al., 2004; Saccani and Photiades, 2005), as testified by the occurrence of Middle to Upper Triassic N-MORBs in the Mirdita zone of Albania (Chiari et al., 1996; Bortolotti et al., 1996; 2004a; 2006), and in the Argolis area of Greece (Bortolotti et al., 2003; Saccani et al., 2003). The Middle-Late Triassic age of N-MORBs form the Fourka Unit (Fig. 8) further support this conclusion. In addition, The oldest MORB sequence from this Unit (section 5, Fig. 8), being the oldest age up to now determined for N-MORB rocks in the Hellenides, provides new constraints for the early oceanization phase in this area, as it indicates that N-MORB crust was already forming during late Anisian-early Ladinian times.

At this stage, enriched transitional to alkaline basalts may have erupted either onto the passive continental realms or in oceanic islands (Pe-Piper, 1998). Although no age data are available for the alkaline rocks included within the Agoriani Mélange, it can be postulated that these rocks may have been erupted during this phase and can either be associated to oceanic seamounts or passive continental margin settings.

ACKNOWLEDGEMENTS

This study was supported by funds from the Italian Ministry of University, University of Florence, University of Ferrara, CNR - Istituto di Geoscienze e Georisorse and by the I.G.M.E. of Athens. Renzo Tassinari is gratefully acknowledged for assistance with XRF and ICP-MS analyses. Many thanks go to P. Dumitrica and E. Piluso for their helpful revisions.

REFERENCES

Baumgartner P.O., Bartolini A.C., Carter E.S., Conti M., Cortese G., Danelian T., De Wever P., Dumitrica P., Dumitrica-Jud R., Goričan S., Guex J., Hull D.M., Kito N., Marcucci M., Matsuoka A., Murchey B., O'Dogherty L., Savary J., Vishnevskaya V., Widz D. and Yao A., 1995a. Middle Jurassic to Early Cretaceous Radiolarian biochronology of Tethys based on Unitary Associations. In: Middle Jurassic to Lower Cretaceous Radiolaria of Tethys: occurrences, systematics, biochronology. In: Baumgartner P.O. et al. (Eds.), Middle Jurassic to Lower Cretaceous Radiolaria of Tethys: occurrences, systematics, biochronology. Mém. Géol., Lausanne, 23: 1013-1048.

Baumgartner P.O., O'Dogherty L., Goričan S., Dumitrica-Jud R., Dumitrica P., Pillevuit A., Urquhart E., Matsuoka A., Danelian T., Bartolini A.C., Carter E.S., De Wever P., Kito N., Marcucci M. and Steiger T.A., 1995b. Radiolarian catalogue and systematics of Middle Jurassic to Early Cretaceous Tethyan genera and species. In: Baumgartner P.O. et al. (Eds.), Middle Jurassic to Lower Cretaceous Radiolaria of Tethys: occurrences, systematics, biochronology. Mém. Géol., Lausanne, 23: 37-685.

Bébien J., Blanchet R., Cadet J.-P., Charvet J., Chorowicz J., Lapierre H. and Rampnoux J.-P., 1978. Le volcanisme triasique des Dinarides en Yougoslavie: sa place dans l'evolution géotectonique peri-Méditerranéenne. Tectonophysics, 47: 159-176.

Beccaluva L., Coltorti M., Premti I., Saccani E., Siena F. and Zeda O. 1994. Mid-ocean ridge and supra-subduction affinities in the ophiolitic belts from Albania. In: L. Beccaluva (Ed.), Albanian ophiolites: state of the art and perspectives. Ofioliti, 19: 77-96.

Bortolotti V., Carras N., Chiari M., Fazzuoli M., Marcucci M., Photiades A. and Principi G., 2003. Argolis Peninsula in the paleogeographic and geodynamic frame of the Hellenides. Ofioliti, 28: 79-94.

Bortolotti V., Chiari M., Kodra A., Marcucci M., Mustafa F., Prela M., Principi G. and Saccani E., 2006. Triassic MORB magmatism in the southern Mirdita Zone ophiolites (Albania). Ofioliti, 31: 1-9.

Bortolotti V., Chiari M., Kodra A., Marcucci M., Mustafa F., Principi G. and Saccani E., 2004a. New evidences for Triassic MORB magmatism in the Northern Mirdita zone ophiolites (Albania). Ofioliti, 29: 247-250.

Bortolotti V., Chiari M., Marcucci M., Marroni M., Pandolfi L., Principi G. and Saccani E., 2004b. Comparison among the Albanian and Greek ophiolites: in search of constraints for the evolution of the Mesozoic Tethys Ocean. Ofioliti, 29: 19-35.

Bortolotti V., Chiari M., Marcucci M., Photiades A., Principi G. and Saccani E., 2005. Triassic and Jurassic radiolarian assemblages from the cherts linked to the MOR basalts in the Othrys area (Greece). Ofioliti, 30: 107.

Bortolotti V., Kodra A., Marroni M., Mustafa F., Pandolfi L., Principi G. and Saccani E., 1996. Geology and petrology of ophiolitic sequences in the central Mirdita region (northern Albania). Ofioliti, 21: 3-20.

Bortolotti V. and Principi G., 2005. Tethyan ophiolites and Pangea break-up. The Island Arc, 14: 442-470.

Capedri S., Toscani L., Grandi R., Venturelli G., Papanikolaou D. and Skarpelis N.S., 1997. Triassic volcanic rocks of some type-localities from the Hellenides. Chem. Erde, 57: 257-276.

Celet P., Courtin B. and Ferrière J., 1980. Les ophiolites des Hellénides centrales dans leur contexte géotectonique. In: A. Panayiotou (Ed.), Ophiolites, Proceed. Intern. Ophiolite Symp., Cyprus 1979, Geol. Surv. Dept. Cyprus, p. 360-371.

Chiari M., Di Stefano P. and Parisi G., 2008. New stratigraphic data on the Middle-Late Jurassic biosiliceous sediments from the Sicanian basin, Western Sicily (Italy). Swiss J. Geosci., 101: 415-429.

Chiari M., Marcucci M., Cortese G., Ondrejickova A. and Kodra A., 1996. Triassic radiolarian assemblages in the Rubik area and Cukali zone, Albania. Ofioliti 21: 77-84.

Danelian T. and Robertson A.H.F., 2001. Neotethyan evolution of eastern Greece (Pangodas Mélange, Evia Island) inferred from radiolarian biostratigraphy and the geochemistry of associated extrusive rocks. Geol. Mag., 138: 345-363.

Degnan P.J. and Robertson A.H.F., 2006. Synthesis of the tectonic-sedimentary evolution of the Mesozoic-Early Cenozoic Pindos: evidence from the NW Peloponnese, Greece. In: A.H.F. Robertson and D. Mountrakis (Eds.), Tectonic development of the Eastern Mediterranean Region. Geol. Soc. London Spec. Publ., 260: 467-492.

Dilek Y., Furnes H. and Shallo M., 2007. Suprasubduction zone ophiolite formation along the periphery of Mesozoic Gondwana. Gondwana Res., 11: 453-475.

Doutsos R., Pe-Piper G., Boronkay K. and Koukouvelas I., 1993. Kinematics of the Central Hellenides. Tectonics, 12: 936-953.

Dumitrica P., 1970. Cryptocephalic and cryptothoracic Nassellaria in some Mesozoic deposits of Romania. Rev. Roum. Géol. Géophys. Géogr., sér. Géol., 14 (1): 45-124.

Dumitrica P., 1978. Family Eptingidae n. fam., ext. Nassellaria (Radiolaria) with sagittal ring. Dari Seama, Inst. Geol. Geofiz., Bucuresti, 64: 57-74.

Dumitrica P. and Dumitrica-Jud R., 2005: *Hexasaturnalis nakasekoi* nov. sp., a Jurassic saturnalid radiolarian species frequently confounded with *Hexasaturnalis suboblongus* (Yao). Rev. Micropal., 48: 159-168.

Feng Q.L., Zhang Z.J. and Ye M., 2001. Middle Triassic radiolarian fauna from southwest Yunnan, China. Micropal., 47 (3): 173-204.

Ferrière J., 1975. Sur la signification des séries du massif de l'Othrys (Grèce continentale orientale): la zone isopique maliaque. Ann. Soc. Géol. Nord., 96 (2): 121-134.

Ferrière J., 1982. Paléogéographie et tectoniques superposées dans les Hellénides internes: les massifs de l'Othrys et du Pelion (Grèce continentale). Soc. Géol. Nord, Publ., 8, 970 pp.

Ferrière J., Bertrand J., Simantov J. and De Wever P., 1988. Comparaison entre les formations volcano-détritiques ("Mélanges") du Malm des Héllénides internes (Othrys, Eubée): implications géodynamiques. Bull. Geol. Soc. Greece, 20: 223-235.

Frey F.A. and Clague D.A., 1983. Geochemistry of diverse basalt types from Loihi seamount, Hawaii. Earth Planet. Sci. Lett., 66: 337-355.

Goričan S. and Buser S., 1990. Middle Triassic radiolarians from Slovenia (Yugoslavia). Geologija, Ljubljana, 31-32: 133-197.

Goričan Š., Halamić J., Grgasović T. and Kolar-Jurkovšek T., 2005. Stratigraphic evolution of Triassic arc-backarc system in northwestern Croatia. Bull. Soc. Géol. France, 176 (1): 3-22.

Haase K.M. and Devey C.W., 1996. Geochemistry of lavas from the Ahu and Tupa volcanic fields, Easter hotspot, southeast Pacific: implications for intraplate magma genesis near a spreading axis. Earth Planet. Sci. Lett., 137: 129-143.

Haase K.M., Stoffers P. and Garbe-Schonberg C.D., 1997. The petrogenetic evolution of lavas from Easter Island and neighbouring Seamounts, near-ridge hotspot volcanoes in the SE Pacific. J. Petrol., 38: 785-813.

Kozur H. and Mostler H., 1994. Anisian to Middle Carnian Radiolarian zonation and description of some stratigraphically important Radiolarians. Geol. Paläont. Mitt. Innsbruck, Sond. 3: 39- 255.

Jackson M.L., 1958. Soil chemical analysis, Prentice-Hall, 498 pp.

Jones G. and Robertson A.H.F., 1991. Tectono-stratigraphy and evolution of the Mesozoic Pindos ophiolite and related units, northwestern Greece. J. Geol. Soc. London, 148: 267-288.

Lachance G.R. and Trail R.J., 1966. Practical solution to the matrix problem in X-ray analysis. Can. Spectr., 11: 43-48.

Lahm B., 1984. Spumellarienfaunen (Radiolaria) aus dem mitteltriassischen Buchensteiner - Schichten von Recoaro (Norditalien) und den obertriassischen Reiflingerkalken von Grossleifling (Österreich) - Systematic - Stratigraphie. Münchner Geowiss. Abh., Reihe A, Geol. Paläont., München, 1: 1-161.

Lipman P.W., Clague D.A., Moore J.G. and Holcomb R.T., 1989. South Arch volcanic field - newly identified young lava flows on the sea floor south of the Hawaiian Ridge. Geology, 17: 611-614.

Marcucci M., Kodra A., Pirdeni A. and Gjata T., 1994. Radiolarian assemblages in the Triassic and Jurassic cherts of Albania. Ofioliti 19: 105-115.

Pearce J.A., 1982. Trace element characteristics of lavas from destructive plate boundaries. In: R.S. Thorpe (Ed.), Andesites. Wiley and Sons, New York, p. 525-548.

Pearce J.A., 1983. Role of the sub-continenetal lithosphere in magma genesis at active continental margin. In: C.J. Hawkesworth and M.J. Norry (Eds.), Continental basalts and mantle xenoliths. Shiva Publ. Co., Nantwich, p. 230-249.

Pearce J.A. and Norry M.J., 1979. Petrogenetic implications of Ti, Zr, Y, and Nb variations in volcanic rocks. Contrib. Mineral. Petrol., 69: 33-47.

Pe-Piper G., 1998. The nature of Triassic extension-related magmatism in Greece: Evidence from Nd and Pb isotope geochemistry. Geol. Mag., 135: 331-348.

Pe-Piper G. and Piper D.J.W., 2002. The igneous rocks of Greece. The anatomy of an orogen. Gebruder Borntraeger, Berlin, 573 pp.

Pessagno E.A. and Newport R.L., 1972. A technique for extracting Radiolaria from radiolarian cherts. Micropal., 18 (2): 231-234.

Prela M., Chiari M. and Marcucci M., 2000. Jurassic radiolarian biostratigraphy of the sedimentary cover of ophiolites in the Mirdita area, Albania: new data. Ofioliti, 25: 55-62.

Ramovs A and Goričan S., 1995. Late Anisian - Early Ladinian radiolarians and conodonts from Smarna Gora near Ljubljana, Slovenia. Razprave 4, Razreda Sazu, 36 (9): 179-221.

Robertson A.H.F., 2002. Overview of the genesis and emplacement of Mesozoic ophiolites in the Eastern Mediterranean Tethyan region. Lithos, 65: 1-67.

Robertson A.H.F., Dixon J.E., Brown S., Collins A., Morris A., Pickett E., Sharp I. and Ustaömer T., 1996. Alternative tectonic models for the Late Paleozoic-Early Tertiary deveolpment of Tethys in the Earstern Mediterranean region. In: A.Morris and D.H. Tarling (Eds.), Paleomagnetism and tectonics of the Mediterranean Region. Geol. Soc., London Spec. Publ., 105: 239-263.

Robertson A.H.F. and Shallo M., 2000. Mesozoic-Tertiary tectonic evolution of Albania in its regional Eastern Mediterranean context. Tectonophysics, 316: 197- 214.

Rocchi S., Mazzotti A., Marroni M., Pandolfi L., Costantini P., Bertozzi G., di Biase D., Federici F. and Goumbo Lo P., 2007a. Detection of Miocene saucer-shaped sills (offshore Senegal) via integrated interpretation of seismic, magnetic and gravity data. Terra Nova, 19: 232-239.

Rocchi S., Marroni M., Pandolfi L., Mazzotti A. and di Biase D., 2007b. Delayed magmatism and tectonic activity at "passive" margins. Proceed. VI Forum italiano Scienze della Terra, Geoitalia 2007, p. 140.

Ross J.V. and Zimmerman J., 1996. Comparison of evolution and tectonic significance of the Pindos and Vourinos ophiolite suite, northern Greece. Tectonophysics, 256: 1-15.

Saccani E., Beccaluva L., Coltorti M. and Siena F., 2004. Petrogenesis and tectono-magmatic significance of the Albanide-Hellenide ophiolites. Ofioliti, 29: 77-95.

Saccani E. and Photiades A., 2005. Petrogenesis and tectono-magmatic significance of volcanic and subvolcanic rocks in the Albanide-Hellenide ophiolitic mélanges. In: Y. Dilek, Y. Ogawa, V. Bortolotti and P. Spadea (Eds.), Evolution of ophiolites in convergent and divergent plate boundaries, The Island Arc, 14: 494-516.

Saccani E., Photiades A. and Padoa E., 2003. Geochemistry, petrogenesis and tectono-magmatic significance of volcanic and subvolcanic rocks from the Koziakas Mélange (Western Thessaly, Greece). Ofioliti, 28: 43-57.

Sashida K., Kamata Y., Adachi S. and Munasri, 1999. Middle Triassic radiolarians from West Timor, Indonesia. J. Paleont., 73 (5): 765-786.

Saunders A.D., Norry M.J. and Tarney J., 1988. Origin of MORB and chemically-depleted mantle reservoirs: Trace element constraints. In: M.A. Menzies and K.G. Cox (Eds.), Oceanic and continental lithosphere: Similarities and differences. J. Petrol., Spec. Vol.: 414-445.

Sharp I.R. and Robertson A.H.F., 2006. Tectonic-sedimentary evolution of the western margin of the Mesozoic Vardar Ocean: evidence from the Pelagonian and Almopias zones, northern Greece. In: A.H.F. Robertson and D. Mountrakis (Eds.), Tectonic development of the eastern Mediterranean region. Geol. Soc. London Spec. Publ., 260: 373-412.

Shervais J.W., 1982. Ti-V plots and the petrogenesis of modern ophiolitic lavas. Earth Planet. Sci. Lett., 59: 101-118.

Sun S.-S. and McDonough W.F., 1989. Chemical and isotopic-systematics of oceanic basalts: implications for mantle composition and processes. In: A.D. Saunders and M.J. Norry (Eds.), Magmatism in the ocean basins. Geol. Soc. London Spec. Publ., 42: 313-345.

Tekin U.K., 1999. Biostratigraphy and systematics of Late Middle to Late Triassic radiolarians from the Taurus Mountains and Ankara region, Turkey. Geol. Paläont. Mitt. Innsbruck, Sonderbd., 5: 1-296.

Tekin U.K and Bedi Y., 2007. Ruesticyrtiidae (Radiolaria) from the middle Carnian (Late Triassic) of Köseyahya Nappe (Elbistan, eastern Turkey). Geol. Carpathica, 2: 153-167.

Tekin U.K. and Mostler H., 2005. Late Ladinian (Middle Triassic) Spumellaria (Radiolaria) from the Dinarides of Bosnia and Herzegovina. Riv. It. Paleont. Strat., 111 (1): 21-43.

Wood D.A., 1980. The application of a Th-Hf-Ta diagram to problems of tectonomagmatic classification and to establishing the nature of crustal contamination of basaltic lavas of the British Tertiary volcanic province. Earth Planet. Sci. Lett., 50: 11-30.

Received, August 6, 2008.
Accepted, November 17, 2008

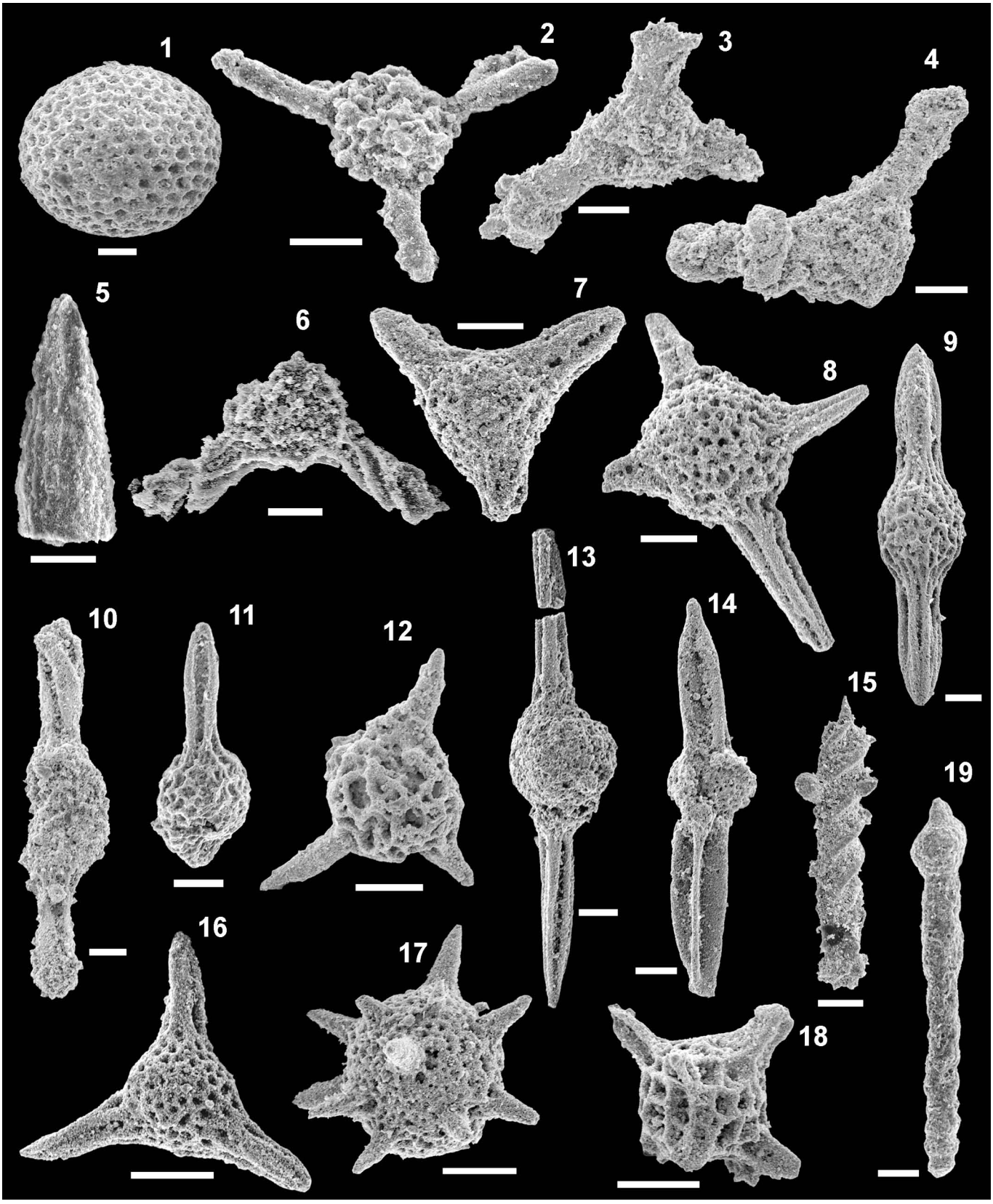

Plate 1 - Middle-Late Triassic Radiolarians. Photos taken with the scanning electron microscope (SEM). Scale bars: 50 μm. 1) *Archaeocenosphaera* sp., GR104. 2) *Capnodoce* sp., GR98. 3) *Capnuchosphaera* sp., GR91. 4) *Capnuchosphaera* (?) sp., GR314. 5) *Corum* (?) sp., GR97. 6) *Cryptostephanidium* (?) sp., GR97. 7) *Eptingium manfredi robustum* Kozur and Mostler, GR104. 8) *Parasepsagon* sp. cf. *P. tetracanthus* Dumitrica, Kozur and Mostler, GR104. 9) *Pseudostylosphaera canaliculata* (Bragin) (=*Pseudostylosphaera coccostyla* (Rüst)), GR104. 10) *Pseudostylosphaera nazarovi* (Kozur and Mostler), GR91. 11) *Pseudostylosphaera* sp. cf. *P. japonica* (Nakaseko and Nishimura), GR104. 12) *Spongostephanidium spongiosum* Dumitrica, GR104. 13) *Spongoxystris koppi* (Lahm), GR104. 14) *Spongoxystris tetrapterum* (Ramovs and Goričan), GR104. 15) *Spongotortilispinus tortilis* (Kozur and Mostler), GR91. 16) *Triassistephanidium* sp. cf. *T. laticornis* Dumitrica, GR104. 17) *Triassospongosphaera* sp., GR104. 18) *Weverisphaera* sp., GR104. 19) *Xiphothecaella* sp. cf. *X. karpenissionensis* (De Wever), GR98.

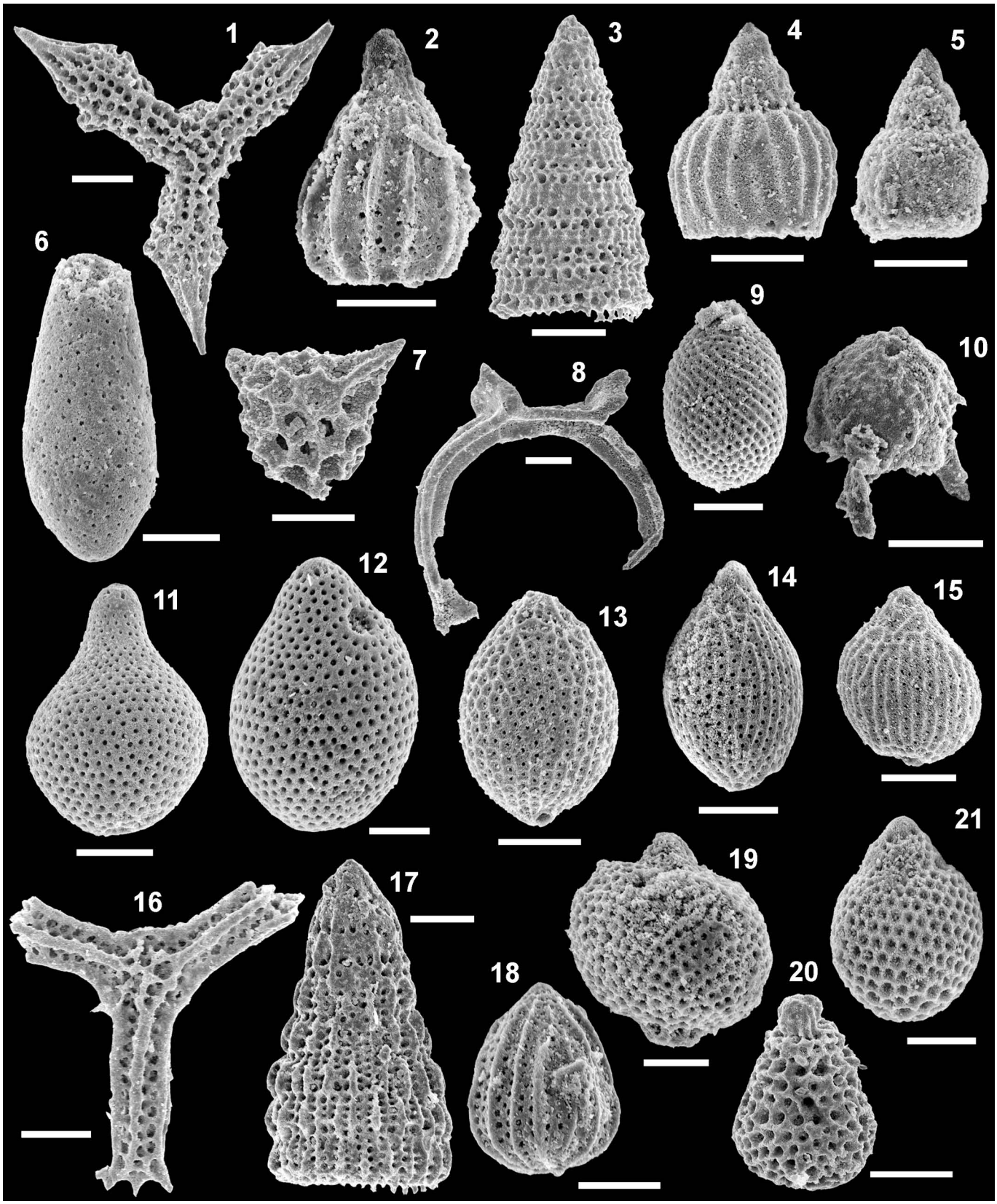

Plate 2 - Middle Jurassic Radiolarians. Photos taken with the scanning electron microscope (SEM). Scale bars: 50 μm. 1) *Angulobracchia* (?) sp., GR110. 2) *Archaeodicyomitra* (?) *amabilis* Aita, GR118. 3) *Dictyomitrella kamoensis* Mizutani and Kido, GR110. 4) *Eucyrtidiellum ptyctum* (Riedel and Sanfilippo), GR118. 5) *Eucyrtidiellum* sp., GR118. 6) *Gongylothorax sakawaensis* Matsuoka, GR110. 7) *Gorgansium* spp. sensu Baumgartner et al. 1995a, GR110. 8) *Hexasaturnalis minor* (Baumgartner), GR110. 9) *Kilinora spiralis* gr. (Matsuoka), GR118. 10) *Saitoum* sp., GR110. 11) *Stichocapsa convexa* Yao, GR110. 12) *Stichocapsa robusta* Matsuoka, GR118. 13) *Striatojaponocapsa conexa* (Matsuoka), GR118. 14) *Striatojaponocapsa plicarum* s.l. Yao, GR110. 15) *Striatojaponocapsa synconexa* O'Dogherty, Goričan and Dumitrica, GR118. 16) *Tritrabs casmaliaensis* (Pessagno), GR110. 17) *Transhuum maxwelli* gr. (Pessagno), GR110. 18) *Unuma gordus Hull,* GR118. 19) *Williriedellum* sp. cf. *W. carpathicum* Dumitrica, GR110. 20) *Zhamoidellum* sp. aff. *Z. argand*i O'Dogherty, Goričan and Dumitrica, GR110. 21) *Zhamoidellum* sp. cf. *Z. ovum* Dumitrica, GR118.